



INTERNSHIP REPORT M1

Theoretical analysis of the relationship  
between semi-phenomenological acoustic  
approaches and self-consistent  
homogenization approaches with  
cylindrical geometry

Jérémie MUZET  
M1 CSMI

Tutor : M. Clément PIEGAY  
Researcher in material acoustics

1 June 2021 — 4 August 2021



## *Special thanks to :*

*My thanks go to the whole acoustic group directed by David ECOTIERE, within the Regional Laboratory of Strasbourg of Cerema.*

*I would like to thank more particularly Clément PIEGAY, my tutor at Cerema, who allowed me to carry out this internship and who was always available to answer my questions and to guide me when necessary.*

*I would like to thank again David ECOTIERE and Clément PIEGAY for their proposal to extend the internship which allowed me to deepen my work.*

*Finally I would like to thank the Regional Laboratory of Strasbourg of Cerema for their welcome and their kindness during my internship.*



# Contents

<b>1</b>	<b>Introduction &amp; Context</b>	<b>4</b>
1.1	Context	4
1.2	Presentation of the company	4
1.3	Internship Subject	5
1.3.1	Tools	5
1.4	Presentation of the modelling approach used	6
1.4.1	The self-consistent homogenization method (SCM)	6
1.4.2	Solutions of the cylindrical SCM model	7
1.4.3	Parameters related to visco-inertial effects and thermal effects	9
<b>2</b>	<b>Modified Bessel functions &amp; first approaches</b>	<b>11</b>
2.1	Modified Bessel functions	11
2.1.1	Low Frequency	11
2.1.2	High Frequency	14
2.2	First approach using the Limiting forms for small arguments method	16
2.2.1	Removing the indeterminate form of the tortuosity for low frequency signals.	16
2.2.2	First approximation of the resistivity.	19
2.3	Verification of the homogeneity of visco-inertial dynamic permeability expressions	22
<b>3</b>	<b>Permeabilities &amp; Results</b>	<b>23</b>
3.1	Determination of dynamic visco-inertial permeabilities	23
3.1.1	Flow approach	23
3.1.2	Pressure approach	24
3.1.3	Approach with the zero vorticity hypothesis	25
3.2	Low Frequency Signal	25
3.2.1	Flow Approach	26
3.2.2	Approach with the zero vorticity hypothesis	26
3.2.3	Pressure Approach	27
3.2.4	Dynamic permeability related to acoustic dissipation by thermal effects	28
3.3	High Frequency Signal	30
3.3.1	Flow Approach	30
3.3.2	Approach with the zero vorticity hypothesis	30
3.3.3	Pressure Approach	31
3.4	Results and comparison	31
3.4.1	Low Frequency	31
3.4.2	High Frequency	32
<b>4</b>	<b>Conclusion</b>	<b>34</b>
<b>5</b>	<b>Bibliography</b>	<b>35</b>

A List of symbols used	36
B Code A - Removing the indeterminate form	37
C Code B - Determination of dynamic visco-inertial permeabilities	39
D Code C - Low Frequency Signal (Visco-inertial effects)	42
E Code D - Low Frequency Signal (Thermal effects)	43



# Chapter 1

## Introduction & Context

The internship is taking place from the 1st of June until August 4, in the "Unité Mixte de Recherche en Acoustique Environnementale (UMRAE)" of the Cerema Lab of Strasbourg. The internship tutor is Clément Piegay, researcher at the UMRAE.

### 1.1 Context

Bio-based materials are an increasing resource in the market of building isolation, because of the introduction of the concept of environmental performance of construction products in the future Environmental Regulation 2020. Those materials, such as vegetal wool (hemp wool, flax wool, cellulose wadding, ...), have the same acoustic performance as the synthetic ones, like rock wool or glass wool [Glé 2013],[Piegay et al.2018], but are more adapted to environmental preservation.

Those bio-based materials are porous and made of fiber, so while taking into account the specificity of their microstructure, a micro-macro homogenization model based on a cylindrical geometry has recently been developed [Piegay et al.2021]. It is based on a coupling between the homogenization of periodic media (HPM) and the self-consistent homogenization method (SCM). This method leads to a direct analytical relation between macroscopic properties (sound absorption coefficient) and parameters of their microstructure, such as an equivalent fiber radius value.

The issue with this approach is that the relations contain modified Bessel functions of the first kind, which lead to indeterminate forms when calculating the limits at low and high frequencies. However, those limits are needed to determine the specific parameters of material pore network geometry, such as the resistivity and the tortuosity of the material.

### 1.2 Presentation of the company

Cerema, Centre d'Etudes et d'expertise sur les Risques, l'Environnement, la Mobilité et l'Aménagement, is a public establishment with administrative status. It has 2,764 employees working in 21 laboratories in France and 3 technical departments.

It operates on the national territory but also at European level. Indeed, Cerema has participated in about forty European projects since its creation. Generally speaking, Cerema's objective is sustainable development and its desire is to design a better future for all territories.



The 9 fields of action of Cerema are :

- Well-being and reduction of nuisances
- Mobility and transport
- Transport infrastructures
- Land use planning and cohesion
- City and urban strategies
- Energy transition and climate

The Strasbourg Laboratory, which is part of the EST Territorial Directorate, is composed of different groups:

- Geotechnics, Earthworks, Pavements Group
- Engineering structures group
- Building, Construction and Real Estate Group
- Acoustics Group
- Physical Methods Group

## 1.3 Internship Subject

This internship, which constitutes a first introduction to the research environment, aims to establish relationships between characteristic geometric parameters of pore networks within materials with parameters related to their microstructure and fiber morphology.

These parameters are related to the acoustic dissipation phenomena within the materials, represented by intrinsic quantities named visco-inertial dynamic permeability ( $\Pi$ ) and thermal dynamic permeability ( $\Xi$ ).

In the case of fibrous materials, both of these permeabilities can be expressed by mathematical relationships based on a cylindrical geometry. These relations are based on modified Bessel functions of the 1st kind,  $I_n$  and  $K_n$ .

In order to establish the relationships between the pore parameters and the microstructure parameters, it is necessary to use specific configurations of low frequencies ( $f$  tends towards 0) and high frequencies ( $f$  tends towards infinity).

A first step is to study the Bessel functions  $I_n$  and  $K_n$  in order to remove the indeterminacies when calculating the limits of the dynamic permeability expressions.

### 1.3.1 Tools

The programming language Python was used for this internship, especially SymPy, the Python library for symbolic mathematics, as the dynamic permeability expressions are composed of multiple parameters. Moreover, the Wolfram|Alpha engine for computing answers was used to find alternative form for small expressions.

For practical use and information sharing, Overleaf was used to show the progress of the results and Box for the document sharing.

## 1.4 Presentation of the modelling approach used

In this section, the modelling method used to establish the dynamic visco-inertial and thermal permeability relationships is presented.

### 1.4.1 The self-consistent homogenization method (SCM)

This modeling approach is based on a self-consistent homogenization model, which is a mathematical model that allows to obtain direct analytical relationships between the parameters of the microstructure and the macroscopic properties of materials.

It has been used in the case of granular materials (spherical geometry) in [Boutin 2000] and also for the case of fibrous materials (cylindrical geometry) by [Berdichevsky & Cai 1993] but only in static. The dynamic case has been developed in [Piégay 2019].

For the application of this method, it is needed to establish the equations of the behavior of the velocity, pressure and temperature fields at the local scale and develop a generic geometric model. Differential equations are then obtained and solved in order to determine solutions for the three characteristic quantities within the fluid phase.

The solutions of dynamic density obtained by this method depend on several parameters and formulas.

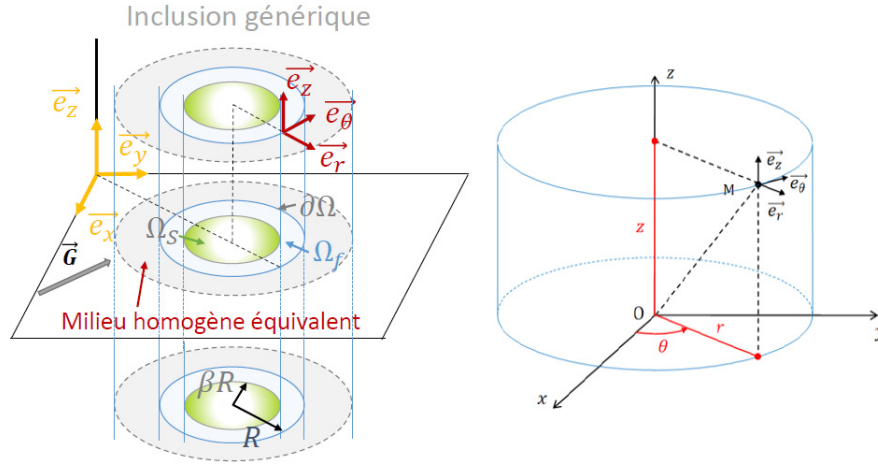


Figure 1.1: Representation of the cylindrical inclusion made of a solid phase included in a fluid phase [Piégay 2019].

First, the fiber radius, which is defined by using the porosity  $\phi$  and the average fiber radius  $R_f$ , is determined by this expression :

$$R = \frac{R_f}{\sqrt{1-\phi}} = \frac{R_f}{\beta}$$

The porosity, noted  $\phi$ , represents the volume of the fluid phase, thus the air, contained in the total volume of the material.

$\beta$  is the homogenization parameter in the cylindrical SCM and can be written as  $\beta = \sqrt{1-\phi}$ .

A sound wave propagating within a material such as plant wools causes a pressure differential that creates a movement of the fluid phase. To characterize the nature of this movement, the viscous boundary layer thickness is defined. Thus, at low frequency when  $\omega$  tends to 0, the wavelengths are very large. The sound wave has more difficulty in penetrating the pores of the material and the flow regime is viscous. Conversely, for high frequencies, the wavelengths are small and generate a faster flow of the fluid, called inertial flow.

The pressure differential within the fluid phase also has an impact on temperature exchanges with the solid phase (thermodynamic evolution). This is why the thermal boundary layer thickness  $\delta_t$  is also defined.

When  $\omega$  tends to 0, there is an isothermal behavior (the fluid moves little, so the temperature remains almost constant) and when  $\omega$  tends to  $\infty$ , there is an adiabatic behavior, the fluid flows quickly and it is considered that exchanges do not have time to occur.

The thickness of the viscous boundary layer is defined by:

$$\delta_v = \sqrt{\frac{\mu}{i\rho_0\omega}}$$

with  $i$  the imaginary unit,  $\mu$  the air shear viscosity ( $1.85 \times 10^{-5} \text{kg.s}^{-1}.\text{m}^{-1}$  at  $25^\circ\text{C}$ ),  $\rho_0$  the mass density of air at rest ( $1.284 \text{kg.m}^{-3}$  at  $25^\circ\text{C}$ ) and  $\omega$  the wave pulsation.

$\omega$  depends on the wave frequency and can be formulated as  $\omega = 2\pi f$ , with  $f$  the wave frequency.

And there is the thickness of the thermal boundary layer :

$$\delta_t = \sqrt{\frac{\lambda_0}{i\rho_0 C_p \omega}}$$

with  $\lambda_0$  the thermal air conductivity ( $0.026 \text{W.m}^{-1}.\text{K}^{-1}$  at  $25^\circ\text{C}$ ),  $\rho_0$  the mass density of air at rest,  $C_p$  the heat capacity of the air at constant pressure and  $\omega$  the wave pulsation.

With all of those parameters and formula, what is left is to introduce the solutions given by the cylindrical SCM.

## 1.4.2 Solutions of the cylindrical SCM model

After solving the differential equation obtained from the modeling method, a solution with constants is obtained. These constants are obtained by using boundary conditions.

One of these boundary conditions corresponds to the conservation of energy between the micro and macro approaches (SCM hypothesis). This boundary condition leads to 2 solutions for the visco-inertial dissipation phenomena. The first one corresponds to the flow approach and the second to the pressure approach.

A third solution is possible, the zero vorticity approach. In his work [Tarnow 1997b], [Tarnow 1997a], V. Tarnow substitutes the hypothesis of conservation of energy by a hypothesis of zero vorticity (but this approach which is valid does not follow from the SCM model).

The SCM model gives three system of five equations, that will be resolved in order to find  $\Pi$  the dynamic permeability for the three approaches of visco-inertial effects in flow, pressure and with the assumption of zero vorticity.

In order to simplify the expression of the following solutions, four last formulas are introduced:

$$\begin{aligned} p &= \frac{R}{\delta_v} \\ q &= \beta p \\ p' &= \frac{R}{\delta_t} \\ q' &= \beta p' \end{aligned}$$

Of the five equation, four are fixed, and the last one depends on the approach :

$$\begin{aligned} \delta_v^2 \left( -\frac{c_0}{(\beta R)^2} + \frac{c_1}{2} \right) + \frac{1}{\delta_v \beta R} (c_2 I_1(q) - c_3 K_1(q)) &= 0 \\ c_1 \delta_v^2 + \frac{c_2}{\delta_v^2} I_0(q) + \frac{c_s}{\delta_v^2} K_0(q) &= 0 \\ \delta_v^2 \left( \frac{c_0}{R^2} - \frac{c_1}{2} \right) - \frac{1}{R \delta_v} (c_2 I_1(p) - c_3 K_1(p)) + \Pi &= 0 \\ 1 - \frac{c_0}{R^2} - \frac{c_1}{2} - \frac{c_2}{\delta_v^3 R} I_1(p) + \frac{c_3}{\delta_v^3 R} K_1(p) &= 0 \end{aligned}$$

#### The dynamic density for the flow approach :

The last equation of the system for the approach is :

$$\frac{1}{2} \left( c_1 \delta_v^2 + \frac{c_2}{\delta_v^2} I_0(p) + \frac{c_s}{\delta_v^2} K_0(p) \right) + \Pi = 0$$

The analytical solution for  $\Pi_v$  is of the form :

$$\Pi_v = \delta_v^2 \left( \frac{R^2 \phi A + 2 \delta_v R (\beta B + C)}{R^2 (1 + \phi) A + 2 \delta_v (-2R\beta^2 E + R\beta F + RC + 8\beta \delta_v G)} \right)$$

with :

$$\begin{aligned} A &= I_0(p)K_0(q) - I_0(q)K_0(p), \\ B &= I_0(p)K_1(q) - I_0(q)K_1(q) + I_1(q)K_0(p) - I_1(q)K_0(q), \\ C &= I_0(p)K_1(p) - I_0(q)K_1(p) + I_1(p)K_0(p) - I_1(p)K_0(q), \\ E &= I_0(q)K_1(p) + I_1(p)K_0(q), \\ F &= I_0(p)K_1(q) + I_0(q)K_1(q) + I_1(q)K_0(p) + I_1(q)K_0(q), \\ G &= -I_1(p)K_1(q) + I_1(q)K_1(p) \end{aligned}$$

#### The dynamic density for the pressure approach :

The last equation of the system for the approach is :

$$-\frac{2\delta_v^2 c_0}{R^3} + \frac{c_2}{\delta_v^3} I_1(p) - \frac{c_2}{\delta_v^2 R} I_2(p) - \frac{c_s}{\delta_v^3} K_1(p) - \frac{c_3}{\delta_v^2 R} K_2(p) = 0$$

The analytical solution for  $\Pi_p$  is of the form :

$$\Pi_p = \delta_v^2 \left( \frac{R^3 \phi E + R^2 \delta_v (2\beta G - \phi A) + 2\delta_v^2 R (\beta B - C)}{\phi R^3 E (R^2 + 4\beta^2 \delta_v) - R^2 \delta_v (2 - \phi) A - 2R \delta_v^2 (C + \beta F) - 2\beta \delta_v (R^2 + 4\delta_v^2) G} \right)$$

### The dynamic density with the assumption of zero vorticity :

The last equation of the system for the approach is :

$$\frac{c_2}{\delta_v^3} I_1(p) - \frac{c_3}{\delta_v^3} K_1(p) = 0$$

The analytical solution for  $\Pi_v$  is of the form :

$$\Pi_z = \delta_v^2 \left( \frac{R\phi E + 2\beta\delta_v G}{R(2 - \phi)E - 2\beta\delta_v G} \right)$$

### The dynamic incompressibility modulus

The thermal permeability is calculated using a system of two equations :

$$\begin{aligned} \delta_t^2 + c_4 I_0(q') + c_5 K_0(q') &= 0 \\ \frac{c_4}{\delta_t} I_1(p') - \frac{c_5}{\delta_t} K_1(p') &= 0 \end{aligned}$$

Solving this system of two equations with two unknowns leads to the following solutions :

$$\begin{aligned} c_4 &= -\frac{\delta_t^2 K_1(p')}{I_0(q') K_1(p') + K_0(q') I_1(p')} \\ c_5 &= -\frac{\delta_t^2 I_1(p')}{I_0(q') K_1(p') + K_0(q') I_1(p')} \end{aligned}$$

Finally, the thermal permeability  $\Xi$  is expressed by the following relation:

$$\Xi = \delta_t^2 \left( 1 - \frac{2\delta_t}{R\phi} [c_4 (I_1(p') - \beta I_1(q')) - c_5 (K_1(p') - \beta K_1(q'))] \right)$$

### 1.4.3 Parameters related to visco-inertial effects and thermal effects

#### Low Frequency

At low frequencies, the viscous phenomena are preponderant on the inertial phenomena. Thus,  $\omega \rightarrow 0$  and  $\lim_{\omega \rightarrow 0} (1/\delta_v) = 0$ .

Based on the work done by Auriault [Auriault et al. 1985] and Boutin [Boutin & Geindreau 2010], the function  $H$  is defined as the inverse of the permeability  $\Pi$ .

$$H = \Pi^{-1}$$

The tortuosity is a dimensionless quantity that accounts for the tortuous path of capillaries in a solid porous medium. The tortuosity, or tortuosity factor, is used to describe the diffusion in this type of medium. It accounts for the reduction that affects the diffusion flow, compared to the value it would have in a straight path.

The static intrinsic permeability  $\Pi_0$  and the low frequency tortuosity  $\alpha_0$  can be estimated from the following relationships:

$$\begin{aligned}\Pi_0 &\simeq \lim_{\omega \rightarrow 0} \operatorname{Re} \left( \frac{1}{H} \right) \\ \alpha_0 &\simeq \lim_{\omega \rightarrow 0} \left( \frac{\phi}{\delta_v^2} H \right)\end{aligned}$$

The static airflow resistance (resistivity) of a material characterizes the ability of a material to resist the flow of a fluid through its structure. It is expressed in  $N.m^{-4}.s$ .

With the static permeability  $\Pi_0$ , it is possible to estimate the resistivity with the following formula :

$$\sigma = \frac{\mu}{\Pi_0}$$

For the thermal effects, with  $\lim_{\omega \rightarrow 0} (1/\delta_t) = 0$ , the static thermal permeability  $\Xi_0$  can be estimated by the following relation :

$$\Xi_0 = \lim_{\omega \rightarrow 0} (\Xi)$$

### High Frequency

At high frequencies, the inertial phenomena are preponderant on the viscous phenomena. Thus,  $\omega \rightarrow +\infty$  and  $\lim_{\omega \rightarrow +\infty} (1/\delta_v) = +\infty$ .

Using the same  $H = \Pi^{-1}$ , the high frequency tortuosity  $\alpha_\infty$  can be estimated with the following formula :

$$\alpha_\infty \simeq \lim_{\omega \rightarrow +\infty} \frac{\mu \phi}{\omega \rho_0} \operatorname{Im}(H)$$

For thermal effects,  $\lim_{\omega \rightarrow +\infty} (1/\delta_t) = +\infty$ .

For a porous medium, it is possible at high frequency to rely on the following relation [Boutin & Geindreau 2010]:

$$\frac{\lambda_f}{j\omega \rho_0 C_p \Xi} \simeq 1 + \sqrt{\frac{M_t \omega}{2 j\omega}}$$

By analogy with visco-inertial effects, [Champoux & Allard 1991] states the following relation, allowing to express the thermal characteristic length  $\Lambda'$  :

$$\sqrt{\frac{M_t \omega}{2 j\omega}} \simeq \frac{2\delta_t}{\Lambda'}$$

$\Lambda'$  can be determined by the following relation:

$$\Lambda' \simeq \lim_{\omega \rightarrow +\infty} 2\delta_t \sqrt{\frac{2 j\omega}{M_t \omega}}$$

## Chapter 2

# Modified Bessel functions & first approaches

### 2.1 Modified Bessel functions

The modified Bessel functions are the backbone of the different relations and formulas in this internship.

$I_{\pm n}(z)$  and  $K_n(z)$  are the solutions of the differential function [Abramowitz & Stegun 1965] :

$$z^2 \frac{d^2 w}{dz^2} + z \frac{dw}{dz} - (z^2 + v^2) w = 0$$

They are called the modified Bessel functions and each is a regular function of  $z$  throughout the  $z$ -plane cut along the negative real axis, and for fixed  $z(\neq 0)$  each is an entire function of  $n$ .

#### 2.1.1 Low Frequency

The modified Bessel functions can be written in these following ascending series forms :

$$I_n(z) = \left(\frac{1}{2}z\right)^n \sum_{k=0}^{\infty} \frac{\left(\frac{1}{4}z^2\right)^k}{k! \Gamma(n+k+1)}$$
$$K_n(z) = \frac{1}{2} \left(\frac{1}{2}z\right)^{-n} \sum_{k=0}^{n-1} \frac{(n-k-1)!}{k!} \left(-\frac{1}{4}z^2\right)^k$$
$$+ (-)^{n+1} \log\left(\frac{1}{2}z\right) I_n(z)$$
$$+ (-)^n \frac{1}{2} \left(\frac{1}{2}z\right)^n \sum_{k=0}^{\infty} \{\psi(k+1) + \psi(n+k+1)\} \frac{\left(\frac{1}{4}z^2\right)^k}{k! \Gamma(n+k+1)}$$

With  $n = 0$  or  $1$  and  $z = p$  or  $z = \beta p$ .

The gamma function  $\Gamma$  correspond to, for  $n > 0$ ,  $\Gamma(n) = (n-1)!$ , and the digamma function  $\psi$  is defined as the derivative of the gamma function  $\psi(n) = \frac{\Gamma'(n)}{\Gamma(n)}$ .

Before using the expressions of I and K into the permeability equations, it is necessary to simplify these series.

**Limiting forms for small arguments.**

At low frequency,  $\omega$ , which is the pulsation of the signal, tends to 0, so both thermal and viscous boundary layer thicknesses,  $\delta_v$  and  $\delta_t$  tend to  $\infty$  and  $p$  ( $p'$ ) or  $\beta p$  ( $\beta p'$ ) tends to 0.

Therefore, the limiting forms for small arguments of the modified Bessel functions [Abramowitz & Stegun 1965] can be used:

$$\begin{aligned} I_0(z) &\underset{0^+}{\sim} 1 \\ I_1(z) &\underset{0^+}{\sim} \frac{z}{2} \\ K_0(z) &\underset{0^+}{\sim} -\log(z) \\ K_1(z) &\underset{0^+}{\sim} \frac{1}{z} \end{aligned}$$

With those forms, the different expressions containing modified Bessel functions can now be simplified quite heavily for low frequency signal :

$$\begin{aligned} A &= I_0(p)K_0(q) - I_0(q)K_0(p) \\ &= -\log(\beta p) + \log(p) \\ &= -\log(\beta) + \log(p) - \log(p) \\ &= \boxed{-\log(\beta)} \end{aligned}$$

$$\begin{aligned} B &= I_0(p)K_1(q) - I_0(q)K_1(p) + I_1(q)K_0(p) - I_1(p)K_0(q) \\ &= \frac{1}{\beta p} - \frac{1}{\beta p} - \frac{\beta p}{2} \log(p) + \frac{\beta p}{2} \log(\beta p) \\ &= \boxed{\frac{\beta p}{2} \log(\beta)} \end{aligned}$$

$$\begin{aligned} C &= I_0(p)K_1(p) - I_0(q)K_1(p) + I_1(p)K_0(p) - I_1(p)K_0(q) \\ &= \frac{1}{p} - \frac{1}{p} - \frac{p}{2} \log(p) + \frac{\beta p}{2} \log(\beta p) \\ &= \frac{p}{2} (\log(\beta p) - \log(p)) \\ &= \boxed{\frac{p}{2} \log(\beta)} \end{aligned}$$

$$\begin{aligned} E &= I_0(q)K_1(p) + I_1(p)K_0(q) \\ &= \frac{1}{p} - \frac{p}{2} \log(\beta p) \underset{0^+}{\sim} \boxed{\frac{1}{p}} \end{aligned}$$



$$\begin{aligned}
F &= I_0(p)K_1(q) + I_0(q)K_1(p) + I_1(q)K_0(p) + I_1(p)K_0(q) \\
&= \frac{1}{\beta p} + \frac{1}{\beta p} - \frac{\beta p}{2} \log(p) - \frac{\beta p}{2} \log(\beta p) \\
&= \frac{2}{\beta p} - \frac{\beta p}{2} (\log(\beta) + 2 \log(p)) \underset{0^+}{\sim} \boxed{\frac{2}{\beta p}}
\end{aligned}$$

$$\begin{aligned}
G &= -I_1(p)K_1(q) + I_1(q)K_1(p) \\
&= -\frac{p}{2\beta p} + \frac{\beta p}{2p} \\
&= \frac{\beta}{2} - \frac{1}{2\beta} \\
&= \frac{\beta^2 - 2}{2\beta} = \boxed{\frac{-\phi}{2\beta}}
\end{aligned}$$

**Asymptotic expansion.**

In the case that it should be necessary to take into account more terms than in the previous approximations, we can also express the modified Bessel functions by asymptotic expansions.

So, the approximations taken for the modified Bessel functions will be the following :

$$\begin{aligned}
I_0(x) &\underset{0^+}{\sim} 1 + \frac{x^2}{4} + o(x^2) \\
I_1(x) &\underset{0^+}{\sim} \frac{x}{2} + o(x^2) \\
K_0(x) &\underset{0^+}{\sim} -\log\left(\frac{x}{2}\right)I_0(x) - \theta + \psi x^2 + o(x^2) \\
K_1(x) &\underset{0^+}{\sim} \frac{1}{x} + \log\left(\frac{x}{2}\right)I_1(x) + \iota x + o(x^2)
\end{aligned}$$

$\theta, \iota$  and  $\psi$  are constant given by the digamma function.

By using those in  $A, B, C, E, F$  and  $G$ , those expressions can be simplified :

$$\begin{aligned}
A &= -\log(\beta) - p^2 \left( \frac{\phi}{4} * \log\left(\frac{p}{2}\right) - \frac{\log(\beta)}{4} \right) + o(p^2) \\
B &= \frac{\beta p}{2} \log(\beta) + o(p^2) \\
C &= \frac{p}{2} \log(\beta) + o(p^2) \\
E &= \frac{1}{p} + p \left( \frac{1-\phi}{4} + \iota + \frac{\theta}{2} - \frac{\log(1-\phi)}{4} \right) + o(p^2) \\
F &= \frac{2}{\beta p} + p \left[ \left( \frac{\log(\beta)}{2} + \frac{\log\left(\frac{\beta}{2}\right)}{2} + 2\iota - \theta \right) \beta + \frac{1}{2\beta} \right] + o(p^2) \\
G &= \frac{-\phi}{2\beta} + o(p^2)
\end{aligned}$$

With  $\iota = 0.03860786$  and  $\theta = 0.57221566$

## 2.1.2 High Frequency

For high frequency signals, the pulsation  $\omega$  tends to  $\infty$ , therefore both thermal and viscous boundary layer thicknesses,  $\delta_v$  and  $\delta_t$  tend to 0 and  $p$  ( $p'$ ) or  $q = \beta p$  ( $q'$ ) tends to  $\infty$ .

In that case, the ascending serie forms shown before can't be simplified like with low frequency signals. In order to solve this problem, another form for the modified Bessel function will be used here.

The modified Bessel functions can be written as polynomial approximations [Abramowitz & Stegun 1965], which take the form:

$$\begin{aligned}
\sqrt{x}e^{-x}I_0(x) &= 0.39894228 + 0.01328592(3.75/x)^1 + 0.00225319(3.75/x)^2 \\
&\quad - 0.00157565(3.75/x)^3 + 0.00916281(3.75/x)^4 - 0.02057706(3.75/x)^5 \\
&\quad + 0.02635537(3.75/x)^6 - 0.01647633(3.75/x)^7 + 0.00392377(3.75/x)^8 + \varepsilon
\end{aligned}$$

$$\begin{aligned}
\sqrt{x}e^{-x}I_1(x) &= 0.39894228 - 0.03988024(3.75/x)^1 - 0.00362018(3.75/x)^2 \\
&\quad + 0.00163801(3.75/x)^3 - 0.01031555(3.75/x)^4 + 0.02282967(3.75/x)^5 \\
&\quad - 0.02895312(3.75/x)^6 + 0.01787654(3.75/x)^7 - 0.00420059(3.75/x)^8 + \varepsilon
\end{aligned}$$

$$\begin{aligned}
\sqrt{x}e^xK_0(x) &= 1.25331414 - 0.07832358(2/x)^1 + 0.02189568(2/x)^2 \\
&\quad - 0.01062446(2/x)^3 + 0.00587872(2/x)^4 - 0.00251540(2/x)^5 \\
&\quad + 0.00053298(2/x)^6 + \varepsilon
\end{aligned}$$

$$\begin{aligned}
\sqrt{x}e^xK_1(x) &= 1.25331414 + 0.23498619(2/x)^1 - 0.03655620(2/x)^2 \\
&\quad + 0.01504268(2/x)^3 - 0.00780353(2/x)^4 + 0.00325614(2/x)^5 \\
&\quad - 0.00068245(2/x)^6 + \varepsilon
\end{aligned}$$

In order to simplify those expressions, it is possible to write all of them with  $o\left(\frac{e^x}{x\sqrt{x}}\right)$ .

$$\begin{aligned} I_0(x) &\underset{+\infty}{\sim} \frac{e^x}{\sqrt{x}} \left( i_1 + \frac{i_2}{x} \right) + o\left(\frac{e^x}{x\sqrt{x}}\right) \\ I_1(x) &\underset{+\infty}{\sim} \frac{e^x}{\sqrt{x}} \left( i_1 - \frac{i_3}{x} \right) + o\left(\frac{e^x}{x\sqrt{x}}\right) \\ K_0(x) &\underset{+\infty}{\sim} \frac{e^{-x}}{\sqrt{x}} \left( k_1 - \frac{k_2}{x} \right) + o\left(\frac{e^x}{x\sqrt{x}}\right) \\ K_1(x) &\underset{+\infty}{\sim} \frac{e^{-x}}{\sqrt{x}} \left( k_1 + \frac{k_3}{x} \right) + o\left(\frac{e^x}{x\sqrt{x}}\right) \end{aligned}$$

with

$i_1$	$i_2$	$i_3$	$k_1$	$k_2$	$k_3$
0.39894228	0.0498222	0.1495509	1.25331414	0.15664716	0.46997238

Then, when it is inserted in the different expressions using the modified Bessel functions, it gives :

$$\begin{aligned} A &= \frac{e^{(1-\beta)p}}{\sqrt{\beta p}} i_1 k_1 + o\left(\frac{e^p}{p\sqrt{p}}\right) \\ B &= \frac{e^{(1-\beta)p}}{\sqrt{\beta p}} i_1 k_1 + o\left(\frac{e^p}{p\sqrt{p}}\right) \\ C &= -\frac{e^{(1-\beta)p}}{\sqrt{\beta p}} i_1 k_1 + o\left(\frac{e^p}{p\sqrt{p}}\right) \\ E &= \frac{e^{(1-\beta)p}}{\sqrt{\beta p}} i_1 k_1 + o\left(\frac{e^p}{p\sqrt{p}}\right) \\ F &= \frac{e^{(1-\beta)p}}{\sqrt{\beta p}} i_1 k_1 + o\left(\frac{e^p}{p\sqrt{p}}\right) \\ G &= -\frac{e^{(1-\beta)p}}{\sqrt{\beta p}} i_1 k_1 + o\left(\frac{e^p}{p\sqrt{p}}\right) \end{aligned}$$

Thus  $A = B = -C = E = F = -G$ .

## 2.2 First approach using the Limiting forms for small arguments method

### 2.2.1 Removing the indeterminate form of the tortuosity for low frequency signals.

My first approach of the problem was to work directly on the low frequency tortuosity, in order to remove the indeterminate form.

$$\alpha_0 = \lim_{\omega \rightarrow 0} \left( \frac{\phi}{\delta_v^2} H \right)$$

With the previous [limiting forms for small arguments](#), the limits of the different 'Bessel-based' expressions can be expressed by these following relationships :

$$\begin{aligned} A &\longrightarrow \log(\beta) \\ B &\longrightarrow 0 \\ C &\longrightarrow 0 \\ E &\longrightarrow \pm\infty \\ F &\longrightarrow \pm\infty \\ G &\longrightarrow \frac{-\phi}{2\beta} \end{aligned}$$

However, if those limits are used directly in the tortuosity expressions, the result is an indeterminate form.

Instead, replacing the expressions by their approximations using the limiting form seems much more relevant.

#### Flow approach.

For the tortuosity, [the dynamic visco-inertial permeability](#) is the main argument.

With this expression, the tortuosity can be expressed [Auriault et al. 1985], [Boutin & Geindreau 2010] by :

$$\begin{aligned} \alpha_0 &= \lim_{\omega \rightarrow 0} \left( \frac{\phi}{\delta_v^2} H \right) \\ &= \lim_{\omega \rightarrow 0} \left( \frac{\phi}{\delta_v^2 \Pi_v} \right) \\ &= \lim_{\omega \rightarrow 0} \left( \frac{R^2 \phi (1 + \phi) A - 4\delta_v R \phi \beta^2 E + 2\delta_v R \phi \beta F + 2\delta_v R \phi C + 16\delta_v^2 \phi \beta G}{\delta_v^4 (R^2 \phi A + 2\delta_v R \beta B + 2\delta_v RC)} \right) \end{aligned}$$

In order to avoid indeterminate form, the expression can be break down to small parts and regrouped :

$$\begin{aligned} \alpha_0 &= \lim_{\omega \rightarrow 0} \left( \frac{R^2 \phi (1 + \phi) A - 4\delta_v R \phi \beta^2 E + 2\delta_v R \phi \beta F + 2\delta_v R \phi C + 16\delta_v^2 \phi \beta G}{\delta_v^4 (R^2 \phi A + 2\delta_v R \beta B + 2\delta_v RC)} \right) \\ &= \lim_{\omega \rightarrow 0} \left( \frac{X2}{\delta^4 X1} - \frac{Y1}{X1} + \frac{Y2}{X1} + \frac{X3}{\delta^4 X1} + \frac{Y3}{X1} \right) \end{aligned}$$

with :

$$\begin{aligned}
X1 &= R^2\phi A + 2\delta_v R\beta B + 2\delta_v RC = \frac{R_f(-2R_f\phi\sqrt{1-\phi} - (2-\phi)(\phi-1))\left(-\log\left(\frac{1}{\sqrt{-i}\sqrt{1-\phi}}\right) + \frac{i\pi}{4}\right)}{(1-\phi)^{3/2}} \\
X2 &= R^2\phi(1+\phi)A = \frac{R_f^2\phi\left(4\log\left(\frac{1}{\sqrt{-i}\sqrt{1-\phi}}\right) - i\pi\right)}{4} \\
X3 &= 2\delta_v R\phi C = \frac{R_f^2\phi\left(-4\log\left(\frac{1}{\sqrt{-i}\sqrt{1-\phi}}\right) + i\pi\right)}{4(1-\phi)} \\
Y1(\omega) &= \frac{4\delta_v R\phi\beta^2 E}{\delta_v^4} = \frac{2\omega\phi\rho_0\left(R_f^2\omega\rho_0\left(\log(R_f) + \frac{-\log(\mu)+\log(\omega)+\log(\rho_0)}{2} + \frac{i\pi}{4}\right) + 2i\mu(1-\phi)\right)}{\mu^2\sqrt{1-\phi}} \\
Y2(\omega) &= \frac{2\delta_v R\phi\beta F}{\delta_v^4} \\
&= \frac{\omega\phi_0\left(R_f^2\omega\rho_0\left(2\log(R_f) - \log(\mu) + \log(\omega) + \log(\rho_0) + \log\left(\frac{1}{\sqrt{-i}\sqrt{1-\phi}}\right) + \frac{i\pi}{4}\right) - 2i\mu(-\sqrt{1-\phi}-1)\right)}{\mu^2} \\
Y3(\omega) &= \frac{16\delta_v^2\phi\beta G}{\delta_v^4} = \frac{-8i\omega\phi^2\rho_0}{\mu}
\end{aligned}$$

All of these expressions were calculated using **SimPy** (see [Appendix](#)).

$X1$ ,  $X2$  and  $X3$  don't depend on  $\omega$ , so they act as constants, unlike  $Y1$ ,  $Y2$  and  $Y3$  which all depend on  $\omega$  and all tend to 0 when  $\omega \rightarrow 0$ .

The expressions can now be regrouped and used to recreate the expression of the tortuosity :

$$\begin{aligned}
\alpha_0 &= \lim_{\omega \rightarrow 0} \left( \frac{X2}{\delta^4 X1} - \frac{Y1}{X1} + \frac{Y2}{X1} + \frac{X3}{\delta^4 X1} + \frac{Y3}{X1} \right) \\
&= \frac{X2}{\infty} - \frac{0}{X1} + \frac{0}{X1} + \frac{X3}{\infty} + \frac{0}{X1}
\end{aligned}$$

The tortuosity for low frequency signals with a flow approach is :

$$\alpha_0 = 0$$

### Pressure approach

Once again, the tortuosity expression is taken with [the permeability for the pressure approach](#) :

$$\begin{aligned}
\alpha_0 &= \lim_{\omega \rightarrow 0} \left( \frac{\phi}{\delta_v^2} H \right) \\
&= \lim_{\omega \rightarrow 0} \left( \frac{\phi}{\delta_v^2 \Pi_p} \right) \\
&= \lim_{\omega \rightarrow 0} \left( \frac{\phi^2 R^5 E + 4\beta^2 \delta_v \phi^2 R^3 E - \phi R^2 \delta_v (2-\phi) A - 2\phi R \delta_v^2 C - 2\phi R \delta_v^2 \beta F - 2\phi \beta \delta_v (R^2 + 4\delta_v^2) G}{\delta_v^4 (R^3 \phi E + R^2 \delta_v (2\beta G - \phi A) + 2\delta_v^2 R (\beta B - C))} \right)
\end{aligned}$$

With  $\Delta$  the denominator, the expression can be rewritten as this sum :

$$\frac{\phi^2 R^5 E}{\Delta} + \frac{4\beta^2 \delta_v \phi^2 R^3 E}{\Delta} - \frac{\phi R^2 \delta_v (2-\phi) A}{\Delta} - \frac{2\phi R \delta_v^2 C}{\Delta} - \frac{2\phi R \delta_v^2 \beta F}{\Delta} - \frac{2\phi \beta \delta_v (R^2 + 4\delta_v^2) G}{\Delta}$$

with :

$$\Delta = \delta_v^4(R^3\phi E + R^2\delta_v(2\beta G - \phi A) + 2\delta_v^2R(\beta B - C))$$

The limits when  $\omega \rightarrow 0$  can now be found for each part of the sum :

- $\Delta_1 = \frac{\phi^2 R^5 E}{\Delta} \xrightarrow{\omega \rightarrow 0} 0$
- $\Delta_2 = \frac{4\beta^2 \delta_v \phi^2 R^3 E}{\Delta} \xrightarrow{\omega \rightarrow 0} 0$
- $\Delta_3 = \frac{\phi R^2 \delta_v (2 - \phi) A}{\Delta} \xrightarrow{\omega \rightarrow 0} 0$
- $\Delta_4 = \frac{2\phi R \delta_v^2 C}{\Delta} \xrightarrow{\omega \rightarrow 0} 0$
- $\Delta_5 = \frac{2\phi R \delta_v^2 \beta F}{\Delta} \xrightarrow{\omega \rightarrow 0} 0$
- $\Delta_6 = \frac{2\phi \beta \delta_v (R^2 + 4\delta_v^2) G}{\Delta} \xrightarrow{\omega \rightarrow 0} 0$

All of these limits were calculated using the function `limit()` of **SimPy** (see [Appendix](#)).

Therefore :

$$\lim_{\omega \rightarrow 0} (\Delta_1 + \Delta_2 - \Delta_3 - \Delta_4 - \Delta_5 - \Delta_6) = 0$$

So, like with the flow approach, the low frequency tortuosity is :

$$\alpha_0 = 0$$

### Zero vorticity assumption

The permeability of the approach with the assumption of zero vorticity is :

$$\Pi_z = \delta_v^2 \left( \frac{R\phi E + 2\beta\delta_v G}{R(2 - \phi)E - 2\beta\delta_v G} \right)$$

Once again, the tortuosity expression is taken with [the permeability of the approach with the assumption of zero vorticity](#) :

$$\begin{aligned} \alpha_0 &= \lim_{\omega \rightarrow 0} \left( \frac{\phi}{\delta_v^2} H \right) \\ &= \lim_{\omega \rightarrow 0} \left( \frac{\phi}{\delta_v^2 \Pi_z} \right) \\ &= \lim_{\omega \rightarrow 0} \left( \frac{R\phi(2 - \phi)E - 2\phi\beta\delta_v G}{\delta_v^4 (R\phi E + 2\beta\delta_v G)} \right) \end{aligned}$$

With the same technique used with the pressure approach,  $\Delta$  is the denominator and the expression can be rewritten as this sum :

$$\frac{R\phi(2-\phi)E}{\Delta} - \frac{2\phi\beta\delta_v G}{\Delta}$$

with :

$$\Delta = \delta_v^4 (R\phi E + 2\beta\delta_v G)$$

The limits when  $\omega \rightarrow 0$  can now be found for each part of the sum :

- $\Delta_1 = \frac{R\phi(2-\phi)E}{\Delta} \xrightarrow{\omega \rightarrow 0} 0$
- $\Delta_2 = \frac{2\phi\beta\delta_v G}{\Delta} \xrightarrow{\omega \rightarrow 0} 0$

*All of these limits were calculated using the function `limit()` of **SimPy** (see [Appendix](#)).*

Therefore :

$$\lim_{\omega \rightarrow 0} (\Delta_1 - \Delta_2) = 0$$

So, like with the flow and pressure approach, the low frequency tortuosity is :

$$\alpha_0 = 0$$

## 2.2.2 First approximation of the resistivity.

In order to find the approximation of the resistivity, it was necessary to find the static intrinsic permeability  $\Pi_0$  for every approach. Therefore, the real and imaginary parts of the permeability are to be separated [Auriault et al. 1985], [Boutin & Geindreau 2010], as :

$$\Pi_0 \simeq \lim_{\omega \rightarrow 0} \text{Re} \left( \frac{1}{H} \right) = \lim_{\omega \rightarrow 0} \text{Re}(\Pi)$$

**Flow approach.**

$$\Pi_v = \delta_v^2 \left( \frac{R^2 \phi A + 2\delta_v R(\beta B + C)}{R^2(1+\phi)A + 2\delta_v(-2R\beta^2 E + R\beta F + RC + 8\beta\delta_v G)} \right)$$

Using the simplified expression of  $A$ ,  $B$ ,  $C$ ,  $E$  and  $F$ ,  $\Pi_v$  can be simplified too :  
**Numerator :**

$$\begin{aligned} R^2 \phi A + 2\delta_v R(\beta B + C) &= -R^2 \phi \log(\beta) + \beta^2 R^2 \log(\beta) + R^2 \log(\beta) \\ &= (1 - \phi + \beta^2) R^2 \log(\beta) \\ &= 2\beta^2 R^2 \log(\beta) \\ &= \boxed{2R_f^2 \log(\beta)} \end{aligned}$$

**Denominator :**

$$\begin{aligned}
R^2(1 + \phi)A &= -R^2(1 - \phi) \log(\beta) = -R_f^2 \log(\beta) \\
-4\delta_v R\beta^2 E &= -4\delta_v^2 \beta^2 \\
-4\delta_v R\beta F &= 4\delta_v^2 \\
2\delta_v RC &= R^2 \log(\beta) \\
16\delta_v^2 \beta G &= 8\delta_v^2 (\beta^2 - 1)
\end{aligned}$$

$$\begin{aligned}
R^2(1 - \phi)A + 2\delta_v(-2R\beta^2 E + R\beta F + RC + 8\beta\delta_v G) &= \delta_v^2(4 - 4\beta^2 + 8\beta^2 - 8) + \frac{\phi}{1 - \phi} R_f^2 \log(\beta) \\
&= \boxed{-4\phi\delta_v^2 + \frac{\phi R_f^2 \log(\beta)}{\beta^2}}
\end{aligned}$$

Permeability for the flow approach :

$$\Pi_v = \frac{2R_f^2 \log(\beta)}{-4\phi\delta_v^2 + \frac{\phi R_f^2 \log(\beta)}{\beta^2}}$$

Now, the permeability is simplified and the real part must be found. The imaginary unit is, in this expression, contained in  $\delta_v$  :

$$\delta_v = \sqrt{\frac{\mu}{i\rho_0\omega}}$$

But the only  $\delta_v$  is in the denominator, so in order to solve that,  $H$  is needed :

$$\begin{aligned}
H = \frac{1}{\Pi_v} &= \frac{-4\phi\delta_v^2}{2R_f^2 \log(\beta)} + \frac{\phi R_f^2 \log(\beta)}{2\beta^2 R_f^2 \log(\beta)} \\
&= \boxed{-\frac{2\phi}{R_f^2 \log(\beta)} + i\frac{\phi\rho_0\omega}{2\beta^2\mu}}
\end{aligned}$$

$H$  is defined in a complex form  $a + ib$ , with :

$$\begin{aligned}
a &= -\frac{2\phi}{R_f^2 \log(\beta)} && \text{The real part} \\
b &= \frac{\phi\rho_0\omega}{2\beta^2\mu} && \text{The imaginary part}
\end{aligned}$$

Finally the real part of  $\Pi_v$  can be found, as the real part of  $\frac{1}{H} = \frac{1}{a + ib}$  is  $\frac{a}{a^2 + b^2}$  :



$$\begin{aligned}
Re\left(\frac{1}{H}\right) &= \frac{-\frac{2\phi}{R_f^2 \log(\beta)}}{\frac{4\phi^2}{R_f^4 \log^2(\beta)} + \frac{\phi^2 \rho_0^2 \omega^2}{4\beta^4 \mu^2}} \\
&= -\frac{2\phi}{R_f^2 \log(\beta)} \frac{4R_f^2 \beta^4 \mu^2 \log^2(\beta)}{16\phi^2 \beta^4 \mu^2 + \phi^2 \rho_0^2 R_f^4 \log^2(\beta) \omega^2} \\
&= -\frac{8\beta^4 R_f^2 \mu^2 \log(\beta)}{16\phi \beta^4 \mu^2 + \phi \rho_0^2 R_f^4 \log^2(\beta) \omega^2}
\end{aligned}$$

And now the static intrinsic permeability can be calculated :

$$\begin{aligned}
\Pi_{0v} &= \lim_{\omega \rightarrow 0} \left( Re\left(\frac{1}{H}\right) \right) \\
&= \lim_{\omega \rightarrow 0} \left( -\frac{8\beta^4 R_f^2 \mu^2 \log(\beta)}{16\phi \beta^4 \mu^2 + \phi \rho_0^2 R_f^4 \log^2(\beta) \omega^2} \right) \\
&= \boxed{-\frac{R_f^2 \log(1 - \phi)}{4\phi}}
\end{aligned}$$

And finally the resistivity  $\sigma$ , defined by  $\sigma = \frac{\mu}{\Pi_0}$ , is :

$$\boxed{\sigma = -\frac{4\phi\mu}{R_f^2 \log(1 - \phi)}}$$

**Pressure approach.**

$$\Pi_p = \delta_v^2 \left( \frac{R^3 \phi E + R^2 \delta_v (2\beta G - \phi A) + 2\delta_v^2 R(\beta B - C)}{\phi R^3 E (R^2 + 4\beta^2 \delta_v) - R^2 \delta_v (2 - \phi) A - 2R \delta_v^2 (C + \beta F) - 2\beta \delta_v (R^2 + 4\delta_v^2) G} \right)$$

By using the same method as previously, the result is :

**Numerator :**

$$\begin{aligned}
\phi R^3 E &= \delta_v \phi R^2 \\
2\beta R^2 \delta_v G &= R^2 \delta (\beta^2 - 1) = -R^2 \delta_v \phi \\
-\phi R^2 \delta_v A &= \phi R^2 \delta_v \log(\beta) \\
2\delta_v^2 R \beta B &= \delta_v R^2 \beta^2 \log(\beta) \\
-2\delta_v^2 R C &= -\delta_v R^2 \log(\beta)
\end{aligned}$$

$$\delta_v \phi R^2 - R^2 \delta_v \phi + \phi R^2 \delta_v \log(\beta) + \delta_v R^2 \beta^2 \log(\beta) - \delta_v R^2 \log(\beta) = \boxed{0}$$

**Denominator :**

The denominator is :

$$\boxed{\delta_v (\phi R^2 (R^2 + 1) + (2 - \phi - R^2) \log(\beta) + 4\phi R^2 \delta_v + 4\delta_v^2 (\phi - 1))}$$

Therefore :

$$\begin{aligned}\Pi_{0p} &= \lim_{\omega \rightarrow 0} \operatorname{Re}(\Pi) = \operatorname{Re}(\lim_{\omega \rightarrow 0}(\Pi)) \\ &= \operatorname{Re}\left(\frac{0}{\delta_v(\phi R^2(R^2 + 1) + (2 - \phi - R^2)\log(\beta) + 4\phi R^2\delta_v + 4\delta_v^2(\phi - 1))}\right) \\ &= \boxed{\pm\infty}\end{aligned}$$

Considering the result obtained, it can be seen that the method used does not allow to establish a usable relationship. It is therefore necessary to implement another method.

In addition, the investigations carried out have identified a problem in the expression of the dynamic visco-inertial permeability.

## 2.3 Verification of the homogeneity of visco-inertial dynamic permeability expressions

The unit of all permeabilities is square meters. It can easily be spotted on the static intrinsic permeability for the flow approach :

$$\Pi_{0v} = -\frac{R_f^2 \log(1 - \phi)}{4\phi}$$

$R_f$  is the average fiber radius, so the unit is meter, and  $\phi$  the porosity is unitless. The unit of  $\Pi_0$  is  $m^2$  as it should be.

But for the pressure approach, a homogeneity problem is encountered. Let's break it down :

$$\Pi_p = \delta_v^2 \left( \frac{R^3 \phi E + R^2 \delta_v (2\beta G - \phi A) + 2\delta_v^2 R(\beta B - C)}{\phi R^3 E(R^2 + 4\beta^2 \delta_v) - R^2 \delta_v (2 - \phi) A - 2R\delta_v^2 (C + \beta F) - 2\beta \delta_v (R^2 + 4\delta_v^2) G} \right)$$

If the different parameters are replaced by their unit :

$$\begin{aligned}& m^2 \left( \frac{m^3 E + m^3 (G - A) + 2m^3 (B - C)}{m^3 E(m^2 + m) - m^3 A - m^3 (C + F) - m^3 G} \right) \\ &= m^2 \left( \frac{m^3 E + (G - A) + (B - C)}{m^3 E(m^2 + m) A - (C + F) - G} \right) \\ &= m^2 \left( \frac{E + (G - A) + (B - C)}{E(m^2 + m) A - (C + F) - G} \right)\end{aligned}$$

$A, B, C, E, F$  and  $G$  are unitless, as they only depend of  $\phi$  (and  $\beta$ ) and  $p$ , which is also unitless because  $p = \frac{R}{\delta_v}$  and the unit of  $R$  and  $\delta_v$  are both meter.

So we can clearly see the homogeneity problem and in order to solve it, the best solution is to move the problem one level higher and recalculate the permeabilities.

## Chapter 3

# Permeabilities & Results

### 3.1 Determination of dynamic visco-inertial permeabilities

In order to recalculate the permeabilities of all approaches, the five equations systems in the part [1.3.2](#) will be used.

#### 3.1.1 Flow approach

For the flow approach, this is the system that will be used :

$$\left\{ \begin{array}{l} \delta_v^2 \left( -\frac{c_0}{(\beta R)^2} + \frac{c_1}{2} \right) + \frac{1}{\delta_v \beta R} (c_2 I_1(q) - c_3 K_1(q)) = 0 \\ c_1 \delta_v^2 + \frac{c_2}{\delta_v^2} I_0(q) + \frac{c_3}{\delta_v^2} K_0(q) = 0 \\ \delta_v^2 \left( \frac{c_0}{R^2} - \frac{c_1}{2} \right) - \frac{1}{R \delta_v} (c_2 I_1(p) - c_3 K_1(p)) + \Pi = 0 \\ 1 - \frac{c_0}{R^2} - \frac{c_1}{2} - \frac{c_2}{\delta_v^3 R} I_1(p) + \frac{c_3}{\delta_v^3 R} K_1(p) = 0 \\ \frac{1}{2} \left( c_1 \delta_v^2 + \frac{c_2}{\delta_v^2} I_0(p) + \frac{c_3}{\delta_v^2} K_0(p) \right) + \Pi = 0 \end{array} \right.$$

Only the last equation depend on the approach, the other one are fixed for all systems. In order to resolve this system, the [LU decomposition](#) can be used but a reorganization of the system is needed. It can be written as :

$$Ax = b$$

with :

$$A = \begin{bmatrix} -\frac{\delta_v^2}{(\beta R)^2} & \frac{\delta_v^2}{2} & \frac{I_1(q)}{\delta_v \beta R} & \frac{-K_1(q)}{\delta_v \beta R} & 0 \\ 0 & \delta_v^2 & \frac{I_0(q)}{\delta_v^2} & \frac{K_0(q)}{\delta_v^2} & 0 \\ \frac{\delta_v^2}{R^2} & -\frac{\delta_v^2}{2} & \frac{-I_1(p)}{R \delta_v} & \frac{K_1(p)}{R \delta_v} & 1 \\ \frac{1}{R^2} & \frac{1}{2} & \frac{I_1(p)}{\delta_v^3 R} & \frac{-K_1(p)}{\delta_v^3 R} & 0 \\ 0 & \frac{\delta_v^2}{2} & \frac{I_0(p)}{2 \delta_v^2} & \frac{K_0(p)}{2 \delta_v^2} & 1 \end{bmatrix} \quad x = \begin{bmatrix} c_0 \\ c_1 \\ c_2 \\ c_3 \\ \Pi \end{bmatrix} \quad b = \begin{bmatrix} 0 \\ 0 \\ 0 \\ 1 \\ 0 \end{bmatrix}$$

The permeability for the flow approach is :

$$\Pi_v = \frac{\delta_v^2 (R^2 \phi A + 2R\delta_v(C - \beta B))}{R^2(2 - \phi)A + 2R\delta_v(C + \beta(2B - F)) + 4R\beta^2\delta_v E - 8\beta\delta_v^2 G}$$

### 3.1.2 Pressure approach

For the pressure approach, this is the system that will be used :

$$\left\{ \begin{array}{l} \delta_v^2 \left( -\frac{c_0}{(\beta R)^2} + \frac{c_1}{2} \right) + \frac{1}{\delta_v \beta R} (c_2 I_1(q) - c_3 K_1(q)) = 0 \\ c_1 \delta_v^2 + \frac{c_2}{\delta_v^2} I_0(q) + \frac{c_3}{\delta_v^2} K_0(q) = 0 \\ \delta_v^2 \left( \frac{c_0}{R^2} - \frac{c_1}{2} \right) - \frac{1}{R\delta_v} (c_2 I_1(p) - c_3 K_1(p)) + \Pi = 0 \\ 1 - \frac{c_0}{R^2} - \frac{c_1}{2} - \frac{c_2}{\delta_v^3 R} I_1(p) + \frac{c_3}{\delta_v^3 R} K_1(p) = 0 \\ -\frac{2\delta_v^2 c_0}{R^3} + \frac{c_2}{\delta_v^3} I_1(p) - \frac{c_2}{\delta_v^2 R} I_2(p) - \frac{c_3}{\delta_v^3} K_1(p) - \frac{c_3}{\delta_v^2 R} K_2(p) = 0 \end{array} \right.$$

With the last equation depending on the pressure approach, the [LU decomposition](#) is used, but first a reorganization of the system is needed. It can be written as :

$$Ax = b$$

with :

$$A = \begin{bmatrix} \frac{-\delta_v^2}{(\beta R)^2} & \frac{\delta_v^2}{2} & \frac{I_1(q)}{\delta_v \beta R} & \frac{-K_1(q)}{\delta_v \beta R} & 0 \\ 0 & \delta_v^2 & \frac{I_0(q)}{\delta_v^2} & \frac{K_0(q)}{\delta_v^2} & 0 \\ \frac{\delta_v^2}{R^2} & -\frac{\delta_v^2}{2} & \frac{-I_1(p)}{R\delta_v} & \frac{K_1(p)}{R\delta_v} & 1 \\ \frac{1}{R^2} & \frac{1}{2} & \frac{I_1(p)}{\delta_v^3 R} & \frac{-K_1(p)}{\delta_v^3 R} & 0 \\ \frac{-2\delta_v^2}{R^3} & 0 & \frac{I_1(p)}{\delta_v^3} - \frac{I_2(p)}{\delta_v^2 R} & \frac{-K_1(p)}{\delta_v^3} - \frac{K_2(p)}{\delta_v^2 R} & 0 \end{bmatrix} \quad x = \begin{bmatrix} c_0 \\ c_1 \\ c_2 \\ c_3 \\ \Pi \end{bmatrix} \quad b = \begin{bmatrix} 0 \\ 0 \\ 0 \\ 1 \\ 0 \end{bmatrix}$$

Finally, the permeability is :

$$\Pi_p = \delta_v^2 \frac{-\phi ER^3 + (\phi E'' - 2\beta G)R^2\delta_v + [2(C' + E') - 2E\beta^2 + \beta(F - B) - 2\beta E'] R\delta_v^2 + 4\beta G\delta_v^3}{-(2 - \phi)ER^3 + (\phi E'' + 2\beta G)R^2\delta_v + [2(C' + E') - 2E\beta^2 + \beta(F - B) + 2\beta E'] R\delta_v^2 + 4\beta G\delta_v^3}$$

with :

$$\begin{aligned} E' &= I_1(q)K_2(p) + I_2(p)K_1(q) \\ E'' &= I_2(p)K_0(q) - I_0(q)K_2(p) \\ C' &= I_1(p)K_2(p) - I_1(q)K_2(p) + I_2(p)K_1(p) - I_2(p)K_1(q) \end{aligned}$$

### 3.1.3 Approach with the zero vorticity hypothesis

For the approach with the zero vorticity hypothesis, this is the system that will be used :

$$\left\{ \begin{array}{l} \delta_v^2 \left( -\frac{c_0}{(\beta R)^2} + \frac{c_1}{2} \right) + \frac{1}{\delta_v \beta R} (c_2 I_1(q) - c_3 K_1(q)) = 0 \\ c_1 \delta_v^2 + \frac{c_2}{\delta_v^2} I_0(q) + \frac{c_3}{\delta_v^2} K_0(q) = 0 \\ \delta_v^2 \left( \frac{c_0}{R^2} - \frac{c_1}{2} \right) - \frac{1}{R \delta_v} (c_2 I_1(p) - c_3 K_1(p)) + \Pi = 0 \\ 1 - \frac{c_0}{R^2} - \frac{c_1}{2} - \frac{c_2}{\delta_v^3 R} I_1(p) + \frac{c_3}{\delta_v^3 R} K_1(p) = 0 \\ \frac{c_2}{\delta_v^3} I_1(p) - \frac{c_3}{\delta_v^3} K_1(p) = 0 \end{array} \right.$$

Same as before, the [LU decomposition](#) can be used, but a reorganization of the system is needed. It can be written as :

$$Ax = b$$

with :

$$A = \begin{bmatrix} \frac{-\delta_v^2}{(\beta R)^2} & \frac{\delta_v^2}{2} & \frac{I_1(q)}{\delta_v \beta R} & \frac{-K_1(q)}{\delta_v \beta R} & 0 \\ 0 & \delta_v^2 & \frac{I_0(q)}{\delta_v^2} & \frac{K_0(q)}{\delta_v^2} & 0 \\ \frac{\delta_v^2}{R^2} & -\frac{\delta_v^2}{2} & \frac{-I_1(p)}{R \delta_v} & \frac{K_1(p)}{R \delta_v} & 1 \\ \frac{1}{R^2} & \frac{1}{2} & \frac{I_1(p)}{\delta_v^3 R} & \frac{-K_1(p)}{\delta_v^3 R} & 0 \\ 0 & 0 & \frac{I_1(p)}{\delta_v^3} & \frac{-K_1(p)}{\delta_v^3} & 0 \end{bmatrix} \quad x = \begin{bmatrix} c_0 \\ c_1 \\ c_2 \\ c_3 \\ \Pi \end{bmatrix} \quad b = \begin{bmatrix} 0 \\ 0 \\ 0 \\ 1 \\ 0 \end{bmatrix}$$

And the permeability for this approach is :

$$\Pi_z = \delta_v^2 \left( \frac{R\phi E + 2\beta\delta_v G}{R(2 - \phi)E - 2\beta\delta_v G} \right)$$

## 3.2 Low Frequency Signal

Now that the relationships of the permeabilities are found, it's time to find the static intrinsic permeability  $\Pi_0$  at low frequency signal for all approaches, in order to establish the expression of the resistivity. But for this part, the limiting form for small arguments will not be used as, like previously in the calculation for the pressure approach, the numerator is 0 for some expressions. Therefore, the asymptotic expansions for the modified Bessel functions come into play.

Using [the asymptotic expansions](#) found before, the different expressions will be too big to be calculated by hand. That's why the calculations in this part will be done with SymPy ([See the Appendix for the code](#)).

### 3.2.1 Flow Approach

Using [SymPy](#), this expression is calculated :

```
>>> Pi_v=delta_v**(R**2*phi**A+2*R*delta_v*(C-bet*B))/(R**2*(2-phi)**A+2*R*delta_v*(C+bet*(2*B-F))+4*R*bet**2*delta_v**E-8*bet*delta_v**2*G)
>>> print(simplify(Pi_v))
I*R_f**2*mu*phi*(-2*mu*(phi - 1)**2*log(1 - phi) - (1 - phi)*(-I*R_f**2*omega*rho_0*(phi*(log(R_f) - log(mu)/2 + log(omega)/2 + log(rho_0)/2 + log(1/sqrt(-I)*sqrt(1 - phi)))) - log(2)) + log(1 - phi)/2) + 2*mu*(phi - 1)*log(1 - phi))/((1 - phi)*(R_f**2*omega*rho_0*(phi - 2)*(I*R_f**2*omega*rho_0*(phi*(log(R_f) - log(mu)/2 + log(omega)/2 + log(rho_0)/2 + log(1/sqrt(-I)*sqrt(1 - phi)))) - log(2)) + log(1 - phi)/2) + 2*mu*(1 - phi)*log(1 - phi)) - 4*mu*(phi - 1)**2*(R_f**2*omega*rho_0*(4*iota - phi + 2*theta - log(1 - phi)/2 + 1) + 4*I*mu*phi + 4*I*mu*(1 - phi)) + 4*mu*(phi - 1)*(R_f**2*omega*rho_0*(1 - phi)*log(1 - phi) + R_f**2*omega*rho_0*(2*(1 - phi)*(2*iota - theta + log(1 - phi)/2) + 1) - R_f**2*omega*rho_0*log(1 - phi)/2 - 4*I*mu*(1 - phi))))
```

Figure 3.1: Permeability with flow approach.

As we have seen previously, the resistivity is expressed as a function of  $\Pi_0$ , the limit of the real part of  $\Pi$ . It is possible to use an equivalence relation for the numerator and the denominator of this expression, as if  $f \sim g$  and  $a \sim b$ , then  $f/a \sim g/b$ .

With the low frequency signal,  $\omega \rightarrow 0$ , so all parts where  $\omega$  is present can be removed.

For the numerator :

$$\underset{0+}{\sim} iR_f^2\mu(-2\mu(2-\phi)(\phi-1)^2\log-1\phi)2\phi(1-\phi)^2\mu\log(1-\phi))$$

For the denominator :

$$\underset{0+}{\sim} 16i\mu^2(1-\phi)^2\phi(\phi-1)$$

There is an imaginary unit in the numerator and the denominator, so the equivalence is real and the result is :

$$\begin{aligned} \Pi_{0v} &= \frac{iR_f^2\mu(-2\mu(2-\phi)(\phi-1)^2\log-1\phi)2\phi(1-\phi)^2\mu\log(1-\phi))}{16i\mu^2(1-\phi)^2\phi(\phi-1)} \\ &= \boxed{\frac{-R_f^2\log(1-\phi)}{4\phi}} \end{aligned}$$

Eventually, this is the same result as in part 2.2.2.

### 3.2.2 Approach with the zero vorticity hypothesis

The same method is used for this approach :

Using [SymPy](#), this expression is calculated :

```
>>> Pi_z=delta_v**(R*phi**E+2*bet*delta_v*G)/(R*(2-phi)**E-2*B*delta_v*G)
>>> print(simplify(Pi_z))
-I*R_f**2*mu*phi*sqrt(1 - phi)*(4*iota - phi + 2*theta - log(1 - phi)/2 + 1)/(-R_f*sqrt(mu)*sqrt(omega)*phi*sqrt(rho_0)*sqrt(-I)*(phi - 1)*log(1 - phi) - sqrt(1 - phi)*(phi - 2)*(R_f**2*omega*rho_0*(4*iota - phi + 2*theta - log(1 - phi)/2 + 1) + 4*I*mu*(phi - 1)))
```

Figure 3.2: Permeability with flow approach.

Same as before, the parts containing  $\omega$  are removed.

For the numerator :

$$\underset{0+}{\sim} -4iR_f^2\mu\phi\sqrt{(1-\phi)}\left(\frac{1-\phi}{4} + \iota + \frac{\theta}{2} - \frac{\log(1-\phi)}{4}\right)$$

For the denominator :

$$\underset{0^+}{\sim} -4i\sqrt{(1-\phi)}\mu(\phi-2)(\phi-1)$$

There is an imaginary unit in the numerator and the denominator, so the equivalence is real and the result is :

$$\begin{aligned}\Pi_{0z} &= \frac{-4iR_f^2\mu\phi\sqrt{(1-\phi)}\left(\frac{1-\phi}{4} + \iota + \frac{\theta}{2} - \frac{\log(1-\phi)}{4}\right)}{-4i\sqrt{(1-\phi)}\mu(\phi-2)(\phi-1)} \\ &= \boxed{\frac{-R_f^2e\phi}{(\phi-2)(\phi-1)}}\end{aligned}$$

$$\text{with } e = \frac{1-\phi}{4} + \iota + \frac{\theta}{2} - \frac{\log(1-\phi)}{4}.$$

### 3.2.3 Pressure Approach

The pressure approach has the most complicated expression for the permeability, but it contains the expression of the approach with the zero vorticity hypothesis :

$$\Pi_p = \delta_v^2 \frac{\boxed{-\phi ER^3 - 2\beta GR^2\delta_v} + \phi E'' R^2\delta_v + [2(C' + E') - 2E\beta^2 + \beta(F - B) - 2\beta E'] R\delta_v^2 + 4\beta G\delta_v^3}{\boxed{-(2-\phi)ER^3 + 2\beta GR^2\delta_v} + \phi E'' R^2\delta_v + [2(C' + E') - 2E\beta^2 + \beta(F - B) + 2\beta E'] R\delta_v^2 + 4\beta G\delta_v^3}$$

The expressions for  $C'$ ,  $E'$  and  $E''$  are :

$$\begin{aligned}E' &= I_1(q)K_2(p) + I_2(p)K_1(q) \\ E'' &= I_2(p)K_0(q) - I_0(q)K_2(p) \\ C' &= I_1(p)K_2(p) - I_1(q)K_2(p) + I_2(p)K_1(p) - I_2(p)K_1(q)\end{aligned}$$

Using the ascending serie form for modified Bessel functions,  $I_2$  and  $K_2$  can be calculated :

$$\begin{aligned}I_2(z) &= \frac{2}{z^2} + o(z^2) \\ K_2(z) &= \frac{z^2}{4} + o(z^2)\end{aligned}$$

By using SymPy, we can remark that all the expressions in the numerator and denominator which are multiplied by  $\delta_v^2$  and  $\delta_v^3$  cancel each other out, which gives us :

$$\begin{aligned}\Pi_p &\underset{0^+}{\sim} \delta_v^2 \frac{-\phi ER^3 - 2\beta GR^2\delta_v}{-(2-\phi)ER^3 + 2\beta GR^2\delta_v} \\ &= \delta_v^2 \frac{R\phi E + 2\beta\delta_v G}{R(2-\phi)E - 2\beta\delta_v G} = \Pi_z\end{aligned}$$

Therefore :

$$\Pi_{0p} = \Pi_{0z} = \boxed{\frac{-R_f^2e\phi}{(\phi-2)(\phi-1)}}$$

$$\text{with } e = \frac{1-\phi}{4} + \iota + \frac{\theta}{2} - \frac{\log(1-\phi)}{4}.$$

### 3.2.4 Dynamic permeability related to acoustic dissipation by thermal effects

For this part, the [limiting forms for small arguments](#) of the modified Bessel functions are used.

$$\Xi = \delta_t^2 \left( 1 - \frac{2\delta_t^2}{R\phi} [c_4(I_1(p') - \beta I_1(q')) - c_5(K_1(p') - \beta K_1(q'))] \right)$$

with :

$$c_4 = -\frac{\delta_t^2 K_1(p')}{I_0(q')K_1(p') + K_0(q')I_1(p')}$$

$$c_5 = -\frac{\delta_t^2 I_1(p')}{I_0(q')K_1(p') + K_0(q')I_1(p')}$$

Now with the limiting forms for small arguments of the modified Bessel functions, the expressions of  $c_4$  and  $c_5$  can be written :

$$c_4 = -\frac{\delta_t^2 K_1(p')}{I_0(q')K_1(p') + K_0(q')I_1(p')}$$

$$= \frac{-\frac{\delta_t^2}{p'}}{\frac{1}{p'} - \frac{p'}{2} \log(\beta p')}$$

$$= \boxed{\frac{-\delta_t^2}{1 - \frac{p'^2}{2} \log(\beta p')}}$$

$$c_5 = -\frac{\delta_t^2 I_1(p')}{I_0(q')K_1(p') + K_0(q')I_1(p')}$$

$$= \frac{\frac{\delta_t^2 p'}{2}}{\frac{1}{p'} - \frac{p'}{2} \log(\beta p')}$$

$$= \boxed{\frac{-\delta_t^2}{\frac{2}{p'} - p \log(\beta p')}}$$



This gives :

$$\begin{aligned} c_4(I_1(p') - \beta I_1(q')) &= \frac{-\delta_t^2}{1 - \frac{p'^2}{2} \log(\beta p')} \left( \frac{p'}{2} - \frac{\beta^2 p'}{2} \right) \\ &= \boxed{\frac{-\delta_t^2 \phi p'}{2 - p'^2 \log(\beta p')}} \end{aligned}$$

$$\begin{aligned} c_5(K_1(p') - \beta K_1(q')) &= \frac{-\delta_t^2}{\frac{1}{p'} - p \log(\beta p')} \left( \frac{1}{p'} - \frac{\beta}{\beta p'} \right) \\ &= \boxed{0} \end{aligned}$$

Those results are implemented in  $\Xi$  :

$$\begin{aligned} \Xi &= \delta_t^2 \left( 1 - \frac{2\delta_t^2}{R\phi} [c_4(I_1(p') - \beta I_1(q')) - c_5(K_1(p') - \beta K_1(q'))] \right) \\ &= \delta_t^2 \left( 1 - \frac{2}{p'\phi} \frac{-\delta_t^2 \phi p'}{2 - p'^2 \log(\beta p')} \right) \\ &= \boxed{\delta_t^2 \left( 1 + \frac{\delta_t^2}{1 - \frac{p'^2}{2} \log(\beta p')} \right)} \end{aligned}$$

In order to find  $\Xi_0$ , the real part of  $\Xi$  is needed. Using the function `re(Xi)` of [SymPy](#), the program gives this solution :

$$\begin{aligned} Re(\Xi) &= \frac{-2\lambda_0^2 \left( \frac{\pi C_p R_f^2 \rho_0 \omega}{4\lambda_0(1-\phi)} + 2 \right)}{C_p^2 \omega^2 \rho_0^2 \left( \frac{C_p^2 R_f^4 \omega^2 \rho_0^2 \log^2 \left( \frac{R_f \sqrt{C_p \rho_0 \omega}}{\sqrt{\lambda_0}} \right)}{\lambda_0^2 (1-\phi)^2} + \frac{\pi C_p R_f^2 \rho_0 \omega}{4\lambda_0(1-\phi)} + 2 \right)} \\ &= \frac{8\lambda_0^3(\phi-1)(\pi C_p R_f^2 \omega \rho_0 - 8\lambda_0(\phi-1))}{C_p^2 \omega^2 \rho_0^2 [4C_p^2 R_f^4 \omega^2 \rho_0^2 (\log(C_p) + 2\log(R_f) - \log(\lambda_0) + \log(\omega) + \log(\rho_0))^2 + (\pi C_p R_f^2 \omega \rho_0 - 8\lambda_0(\phi-1))^2]} \end{aligned}$$

$$\underset{0^+}{\sim} \frac{\lambda_0^2}{C_p^2 \omega^2 \rho_0^2} = \Xi_0$$

### 3.3 High Frequency Signal

At high frequency, we can write :

- $\delta_v \xrightarrow{\omega \rightarrow \infty} 0$
- $A = B = -C = E = F = -G$

#### 3.3.1 Flow Approach

Based on the second previously expression, we can determine an equivalent relationship when  $\omega$  tends to  $\infty$  for the dynamic visco-inertial permeability :

$$\begin{aligned} \Pi_v &= \frac{\delta_v^2 (R^2 \phi + 2R\delta_v(-1 - \beta))}{R^2(2 - \phi) + 2R\delta_v(-1 + \beta) + 4R\beta^2\delta_v + 8\beta\delta_v^2} \\ &\underset{+\infty}{\sim} \frac{\delta_v^2 R^2 \phi}{R^2(2 - \phi)} = \frac{\delta_v^2 \phi}{(2 - \phi)} \end{aligned}$$

Let's now find  $\text{Im}(H)$  :

$$H = \frac{(2 - \phi)}{\delta_v^2 \phi} = i \frac{\omega \rho_0 (2 - \phi)}{\mu \phi} = i \text{Im}(H)$$

Now for the tortuosity :

$$\begin{aligned} \alpha_{\infty v} &= \lim_{\omega \rightarrow +\infty} \frac{\mu \phi}{\omega \rho_0} \text{Im}(H) \\ &= \lim_{\omega \rightarrow +\infty} \frac{\mu \phi}{\omega \rho_0} \frac{\omega \rho_0 (2 - \phi)}{\mu \phi} \\ &= \boxed{2 - \phi} \end{aligned}$$

#### 3.3.2 Approach with the zero vorticity hypothesis

Based on the same assumptions that for the flow approach, we can write :

$$\begin{aligned} \Pi_z &= \delta_v^2 \left( \frac{R\phi - 2\beta\delta_v}{R(2 - \phi) + 2\beta\delta_v} \right) \\ &\underset{+\infty}{\sim} \frac{\delta_v^2 R\phi}{R(2 - \phi)} = \frac{\delta_v^2 \phi}{(2 - \phi)} \end{aligned}$$

Let's now find  $\text{Im}(H)$  :

$$H = \frac{(2 - \phi)}{\delta_v^2 \phi} = i \frac{\omega \rho_0 (2 - \phi)}{\mu \phi}$$

Now for the tortuosity :

$$\begin{aligned} \alpha_{\infty v} &= \lim_{\omega \rightarrow +\infty} \frac{\mu \phi}{\omega \rho_0} \text{Im}(H) \\ &= \lim_{\omega \rightarrow +\infty} \frac{\mu \phi}{\omega \rho_0} \frac{\omega \rho_0 (2 - \phi)}{\mu \phi} \\ &= \boxed{2 - \phi} \end{aligned}$$

### 3.3.3 Pressure Approach

The expression of the permeability can be simplified using  $\delta_v \xrightarrow{\omega \rightarrow \infty} 0$

$$\Pi_p = \delta_v^2 \frac{\phi ER^3 - 2\beta GR^2 \delta_v + \phi E'' R^2 \delta_v + [2(C' + E') - 2E\beta^2 + \beta(F - B) - 2\beta E'] R \delta_v^2 + 4\beta G \delta_v^3}{-(2 - \phi)ER^3 + 2\beta GR^2 \delta_v + \phi E'' R^2 \delta_v + [2(C' + E') - 2E\beta^2 + \beta(F - B) + 2\beta E'] R \delta_v^2 + 4\beta G \delta_v^3}$$

$$\underset{+\infty}{\sim} \delta_v^2 \frac{-\phi ER^3}{-(2 - \phi)ER^3} = \frac{\delta_v^2 \phi}{(2 - \phi)}$$

Let's now find  $\text{Im}(H)$  :

$$H = \frac{(2 - \phi)}{\delta_v^2 \phi} = i \frac{\omega \rho_0 (2 - \phi)}{\mu \phi}$$

Now for the tortuosity :

$$\begin{aligned} \alpha_{\infty v} &= \lim_{\omega \rightarrow +\infty} \frac{\mu \phi}{\omega \rho_0} \text{Im}(H) \\ &= \lim_{\omega \rightarrow +\infty} \frac{\mu \phi}{\omega \rho_0} \frac{\omega \rho_0 (2 - \phi)}{\mu \phi} \\ &= \boxed{2 - \phi} \end{aligned}$$

## 3.4 Results and comparison

### 3.4.1 Low Frequency

#### Visco-Inertial effects

In the case of the low frequency signals, the most valuable result researched here was the resistivity.

As the static intrinsic permeability  $\Pi_0$  has been found for all approaches, the resistivity is :

$$\sigma = \frac{\mu}{\Pi_0}$$

$$\frac{\sigma_v}{\frac{4\mu\phi}{-R_f^2 \log(1 - \phi)}} \quad \left| \quad \frac{\sigma_p}{\frac{\mu(\phi - 2)(\phi - 1)}{-R_f^2 e\phi}} \quad \right| \quad \frac{\sigma_z}{\frac{\mu(\phi - 2)(\phi - 1)}{-R_f^2 e\phi}}$$

$$\text{with } e = \frac{1 - \phi}{4} + \iota + \frac{\theta}{2} - \frac{\log(1 - \phi)}{4}.$$

Now if the parameters are replaced by the numerical values corresponding to the flax wool's property at 25°C :

- $\mu = 1.85e - 5 \quad (kg.s^{-1}.m^{-1})$
- $\phi = 0.979$
- $R_f = 12.65e - 6 \quad (m)$

and with the different constant of the modified Bessel functions,  $\iota = 0.03860786$  and  $\theta = 0.57221566$ , we have :

$$\frac{\sigma_v}{117187.820230659} \quad \left| \quad \frac{\sigma_p}{3907.99311566433} \quad \right| \quad \frac{\sigma_z}{3907.99311566433}$$

Those values can be compared with the experimental result of Clement Piégay [Piégay 2019] :

Laine	Réf.	$\sigma - p (N.m^{-4}.s)$	$\sigma - v (N.m^{-4}.s)$	$\sigma - z (N.m^{-4}.s)$	$\sigma exp (N.m^{-4}.s)$
Lin	D	5898	7650	6256	5052

Figure 3.3: Resistivity values estimated from the 3 approaches p, v and z from the modeling HAC cylindrical and experimentally characterized resistivity value for flax wool (D) [Piégay 2019]

The result given by the flow approach is very far, so there must be a problem in the expression. This can come from the approximation of the modified Bessel functions.

The result obtained for the pressure approach and the zero vorticity approach gives a result of the same order of magnitude as the experimental value. It is an interesting result, but it should be confirmed by comparing with other experimental values.

### Thermal effects

The results for the static thermal permeability in [Piégay 2019] are as follows :

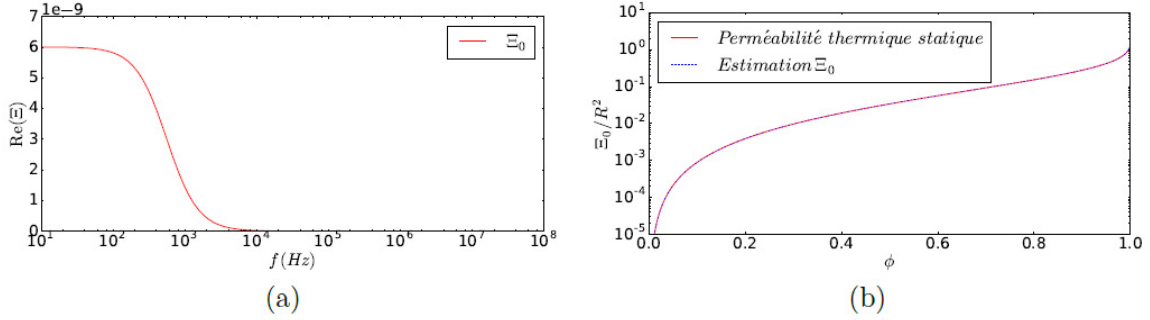


Figure 3.4: (a) Representation of the real part of the thermal permeability as a function of the frequency for flax wool (D), (b) evolution of the thermal permeability value  $\Xi_0/R_2$  as a function of the porosity.

The static thermal permeability found during the internship is :

$$\Xi_0 = \frac{\lambda_0^2}{C_p^2 \omega^2 \rho_0^2}$$

With numerical values, the result doesn't match with Clément work.  $\Xi_0$  does not depend on the porosity  $\phi$ , therefore it is impossible to verify if, when the porosity tends to 0,  $\Xi_0/R_2$  tends to 0 and when it tends to 1,  $\Xi_0/R_2$  tends to 1.

This is maybe due to the use of the limiting form for small arguments instead of the asymptotic expansions for the modified Bessel functions, that were not used because of a lack of time.

### 3.4.2 High Frequency

For the high frequency signal, there is the same tortuosity for all approaches :

$$\frac{\alpha_{\infty v}}{(2 - \phi)} \quad \bigg| \quad \frac{\alpha_{\infty p}}{(2 - \phi)} \quad \bigg| \quad \frac{\alpha_{\infty z}}{(2 - \phi)}$$

Likewise, in [Piégay 2019] the relationship between high frequency tortuosity and porosity is :

$$\alpha_{\infty} = 2 - \phi$$

This figure represents the evolution of the function to which the tortuosity is related as a function of frequency :

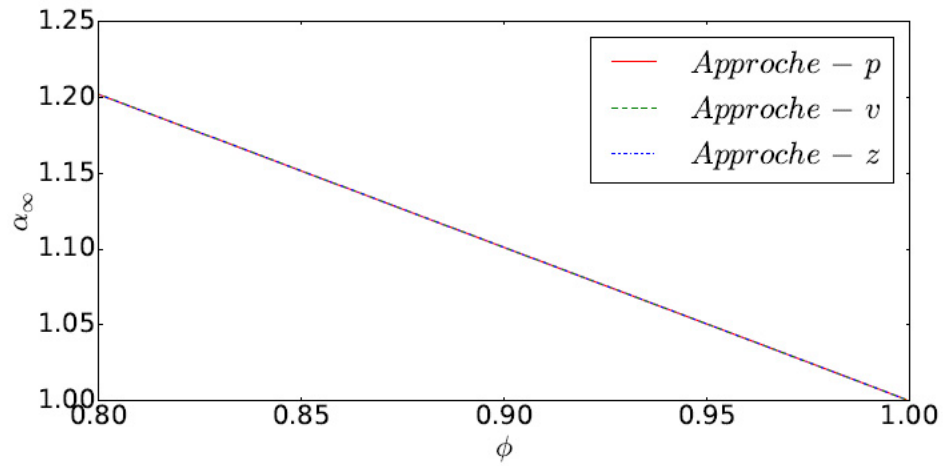


Figure 3.5: Evolution of the values of  $\alpha - p$ ,  $\alpha - v$  and  $\alpha - z$  in relation to the porosity [Piégay 2019].

## Chapter 4

# Conclusion

The internship explored different mathematical methods to find equivalent expressions in 0 and infinity of special Bessel functions.

For the particular case of the internship, which concerns acoustic dissipative phenomena inside fibrous materials, this has allowed to identify the methods on which we can rely.

The internship also allowed to re-establish the expressions of dynamic visco-inertial permeability. By taking a step back, we realize that given the heaviness of the expressions, an error can easily slip in. It is therefore necessary to be very rigorous in the establishment of relations and the resolution of equations. The use of a software of formal calculation seems then essential.

But the limitation of the software used, SymPy, were the reason for the simplification of the modified Bessel functions. It could be interesting, maybe with a more powerful software of formal calculation, to calculate the different permeability expressions using the full expression of the ascending serie form for example.

Regarding the expressions obtained, we have seen that it is necessary to make several checks such as homogeneity, and then to test them with experimental values and results.

Expressions such as high frequency tortuosity for example give results in agreement with experimental results. The internship also allowed to identify that some expressions (like resistivity for the flow approach) could not be validated.

There is still work to be done on some expressions, and there are still relationships to establish for the viscous and thermal characteristic lengths. More validations will also be necessary using other experimental values related to plant wools but also to other fibrous insulators or even other fibrous materials.

During this internship, I was able to discover and apply Bessel's functions, as well as learn to program on SymPy. This introduction to research showed me that there are many approaches to the same problem and that knowing how to adapt to new situations is crucial for this type of work.

## Chapter 5

# Bibliography

- [Abramowitz & Stegun 1965 ] M. Abramowitz et I.A. Stegun .*Handbook of Mathematical Functions*. Dover Publications Inc. 1965.
- [Auriault et al. 1985 ] J-L. Auriault, L. Borne et R. Chambon. *Dynamics of porous saturated media, checking of the generalized law of Darcy*. Journal of the Acoustical Society of America, vol. 77, no. 5, p. 1641–1650, 1985.
- [Boutin & Geindreau 2010 ] C. Boutin et C. Geindreau. *Periodic homogenization and consistent estimates of transport parameters through sphere and polyhedron packings in the whole porosity range*. Physical review E, vol. 82, no. 3, 036313 p., 2010.
- [Berdichevsky & Cai 1993 ] A.L. Berdichevsky et Z. Cai. *Perform permeability predictions by self consistent method and finite element simulation*. Polym. Compos., vol. 14, no. 2, p. 132–143, 1993.
- [Boutin 2000 ] C. Boutin. *Study of permeability by periodic and self-consistent homogenisation*. European Journal of Mechanics - A/Solids, vol. 19, no. 4, p. 603–632, 2000.
- [Champoux & Allard 1991 ] Y. Champoux et J-F. Allard. *Dynamic tortuosity and bulk modulus in air-saturated porous media*. Applied Physics, vol. 70, p. 1975–1979, 1991.
- [Glé 2013 ] P. Glé. *Acoustique des Matériaux du Bâtiment à base de Fibres et Particules Végétales- Outils de Caractérisation, Modélisation et Optimisation*. Thèse de doctorat, INSA de Lyon, 2013.
- [Piégay 2019 ] P. Glé. *Approche Conjointe Acoustique et Thermique pour l’Optimisation des Laines Végétales du Bâtiment*. Thèse de doctorat, Lyon, 2019.
- [Piégay et al. 2018 ] C. Piégay, P. Glé, E. Gourdon, E. Gourlay et S. Marceau. *Acoustical model of vegetal wools including two types of fibers*. Applied Acoustics, vol. 129, p. 36–46, Janvier 2018.
- [Piegay et al. 2021 ] C. Piégay, P. Glé, E. Gourdon, E. Gourlay et S. Marceau. *A self-consistent approach for the acoustical modeling of vegetal wools*. Journal of Sound and Vibration, vol. 495, 115911, Mars 2021.
- [Tarnow 1997a ] V. Tarnow. *Calculation of the dynamic air flow resistivity of fiber materials*. The Journal of the Acoustical Society of America, vol. 102, no. 3, p. 1680–1688, 1997.
- [Tarnow 1997b ] V. Tarnow. *Compressibility of air in fibrous materials*. Journal of the acoustical Society of America, vol. 102, no. 3, p. 1680–1688, 1997.

# Appendix A

## List of symbols used

- $C_p$  : heat capacity of air at constant pressure ( $J.K^{-1}.kg^{-1}$ )
- $f$  : frequency of the wave ( $Hz$ )
- $R$  : radius in cylindrical coordinates ( $m$ )
- $R_f$  : average radius of the fibers ( $m$ )
- $\alpha$  : tortuosity
- $\beta$  : homogenization parameter (cylindrical HAC)
- $\delta_t$  : thickness of the thermal layer ( $m$ )
- $\delta_v$  : thickness of the viscous boundary layer ( $m$ )
- $\Lambda'$  : thermal characteristic length ( $m$ )
- $\lambda_0$  : thermal conductivity ( $W.m^{-1}.K^{-1}$ )
- $\mu$  : shear viscosity ( $Pa.s$ )
- $\Xi$  : thermal dynamic permeability ( $m^2$ )
- $\Xi_0$  : thermal static permeability ( $m^2$ )
- $\Pi$  : dynamic permeability ( $m^2$ )
- $\Pi_0$  : static permeability of the fluid phase ( $m^2$ )
- $\rho_0$  : density of the air at the origin ( $kg.m^{-3}$ )
- $\sigma$  : static resistance to air flow (resistivity) ( $N.m^{-4}.s$ )
- $\phi$  : porosity
- $\omega$  : pulsation of the wave ( $rad.s^{-1}$ )



## Appendix B

# Code A - Removing the indeterminate form

```
1 from sympy import *
2
3 init_session()
4 init_printing()
5
6 from sympy import *
7 import numpy as np
8 import scipy.integrate as integrate
9 import scipy.special as special
10
11 omega = symbols('omega',real=True, positive=True)
12 R_f = symbols('R_f',real=True, positive=True)
13 phi = symbols('phi',real=True, positive=True)
14 rho_0 = symbols('rho_0',real=True, positive=True)
15 mu = symbols('mu',real=True, positive=True)
16 lambda_0 = symbols('lambda_0',real=True, positive=True)
17 C_p = symbols('C_p',real=True, positive=True)
18 delta_v = sqrt(mu/(I*rho_0*omega))
19
20 bet = sqrt(1-phi)
21 R = R_f/bet
22 p = R/delta_v
23 q = p*bet
24
25 A = -log(bet)
26 B = bet*p*log(bet)/2
27 C = p*log(bet)/2
28 E = 1/p
29 F = 2/(bet*p)
30 G = -phi/(2*bet)
31
32 lim_A = limit(A,omega,0)
33 lim_B = limit(B,omega,0)
34 lim_C = limit(C,omega,0)
35 lim_E = limit(E,omega,0)
36 lim_F = limit(F,omega,0)
37 lim_G = limit(G,omega,0)
38
39 print("A->",lim_A," B->",lim_B," C->",lim_C," E->",lim_E," F->",lim_F," G
->",lim_G)
40
41
42
```

```

43 ##### Flow approach
44
45 X1=simplify(2*R**2*phi*A+2*delta_v*(bet*B+C))      #X1
46 X2=simplify(R**2*phi*(1-phi)*A)                   #X2
47 Y1=simplify(4*delta_v*R*phi*bet*E/(delta_v**4))   #Y1(omega)
48 Y2=simplify(2*delta_v*R*phi*bet*F/(delta_v**4))   #Y2(omega)
49 X3=simplify(2*delta_v*phi*R*C)                     #X3
50 Y3=simplify(16*delta_v**2*phi*bet*G/(delta_v**4)) #Y3(omega)
51
52 (Y2+Y3-Y1)/X1
53
54 limit((Y2+Y3-Y1)/X1,omega,0)
55
56 ##### Pressure approach
57
58 PI_p = delta_v**2*( R**3*phi*E + R**2*delta_v*(2*bet*G-phi*A) + 2*delta_v**2*R*(bet
    *B-C) )/( phi*R**3*E*(R**2+4*bet**2*delta_v) - R**2*delta_v*(2-phi)*A - 2*R*
    delta_v**2*(C+bet*F) - 2*bet*delta_v*(R**2+4*delta_v**2)*G )
59
60 limit( phi**2*R**5*E / (delta_v**4*(R**3*phi*E + 2*R**2*delta_v*bet*G-2*R**2*
    delta_v*phi*A+2*delta_v**2*R*bet*B-2*delta_v**2*R*C)), omega, 0 )
61
62 limit( phi**2*R**3*E*4*bet**2*delta_v / (delta_v**4*(R**3*phi*E + 2*R**2*delta_v*
    bet*G-2*R**2*delta_v*phi*A+2*delta_v**2*R*bet*B-2*delta_v**2*R*C)), omega, 0 )
63
64 limit( phi*R**2*delta_v*(2-phi)*A / (delta_v**4*(R**3*phi*E + 2*R**2*delta_v*bet*G
    -2*R**2*delta_v*phi*A+2*delta_v**2*R*bet*B-2*delta_v**2*R*C)), omega, 0 )
65
66 limit( 2*phi*R*delta_v**2*C / (delta_v**4*(R**3*phi*E + 2*R**2*delta_v*bet*G-2*R
    **2*delta_v*phi*A+2*delta_v**2*R*bet*B-2*delta_v**2*R*C)), omega, 0 )
67
68 limit( 2*phi*R*delta_v**2*bet*F / (delta_v**4*(R**3*phi*E + 2*R**2*delta_v*bet*G-2*
    R**2*delta_v*phi*A+2*delta_v**2*R*bet*B-2*delta_v**2*R*C)), omega, 0 )
69
70 limit( 2*phi*R*delta_v*bet*(R**2+4*delta_v**2)*G / (delta_v**4*(R**3*phi*E + 2*R
    **2*delta_v*bet*G-2*R**2*delta_v*phi*A+2*delta_v**2*R*bet*B-2*delta_v**2*R*C)),
    omega, 0 )
71
72 ##### Approach with the zero vorticity hypothesis
73
74 PI_z=delta_v**2*(R*phi*E+2*bet*delta_v*G)/(R*(2-phi)*E-2*B*delta_v*G)
75
76 alpha_0z = phi/(PI_z*delta_v**2)
77
78 limit(alpha_0z, omega,0)

```

Listing B.1: Code A

## Appendix C

# Code B - Determination of dynamic visco-inertial permeabilities

```
1 from sympy import *
2
3 init_session()
4 init_printing()
5
6 from sympy import *
7 import numpy as np
8 import scipy.integrate as integrate
9 import scipy.special as special
10
11 omega = symbols('omega',real=True, positive=True)
12 R_f = symbols('R_f',real=True, positive=True)
13 phi = symbols('phi',real=True, positive=True)
14 rho_0 = symbols('rho_0',real=True, positive=True)
15 mu = symbols('mu',real=True, positive=True)
16 lambda_0 = symbols('lambda_0',real=True, positive=True)
17 C_p = symbols('C_p',real=True, positive=True)
18 delta_v = symbols('delta_v')
19 R = symbols('R',real=True, positive=True)
20 bet = symbols('bet',real=True, positive=True)
21 I0_p= symbols('I0_p')
22 I1_p= symbols('I1_p')
23 K0_p= symbols('K0_p')
24 K1_p= symbols('K1_p')
25 I0_q= symbols('I0_q')
26 I1_q= symbols('I1_q')
27 K0_q= symbols('K0_q')
28 K1_q= symbols('K1_q')
29 I2_p =symbols('I2_p')
30 K2_p=symbols('K2_p')
31 c_0 = symbols('c_0')
32 c_1 = symbols('c_1')
33 c_2 = symbols('c_2')
34 c_3 = symbols('c_3')
35 Pi = symbols('Pi')
36
37
38
39
40
41
42
43
```

```

44 #FLOW
45 #####
46
47 solve_linear_system_LU(Matrix([ [ -delta_v**2/(bet*R)**2, delta_v**2/2, I1_q/(
    delta_v*bet*R), -K1_q/(delta_v*bet*R), 0,0], [0, delta_v**2, I0_q/delta_v**2,
    K0_q/delta_v**2, 0,0], [delta_v**2/R**2, -delta_v**2/2, -I1_p/(R*delta_v), K1_p
    /(R*delta_v), 1,0], [1/R**2, 1/2, I1_p/(delta_v**3*R), -K1_p/(delta_v**3*R),
    0,1], [0, delta_v**2/2, I0_p/(2*delta_v**2), K0_p/(2*delta_v**2), 1,0]]),[c_0,
    c_1,c_2,c_3,Pi])
48
49 Pi_p = (delta_v**2*(I0_p/(2*delta_v**2) - I0_q/(2*delta_v**2))/(I0_q/delta_v**2 -
    2*I1_p/(R*delta_v)) - (delta_v**2*(-I0_q*(delta_v**2/2 + 0.5*delta_v**2/bet**2)
    /delta_v**4 + I1_p/(R*bet**2*delta_v) + I1_q/(R*bet*delta_v))/(I0_q/delta_v**2
    - 2*I1_p/(R*delta_v)) + delta_v**2/bet**2)*(K0_p/(2*delta_v**2) - K0_q/(2*
    delta_v**2) - (I0_p/(2*delta_v**2) - I0_q/(2*delta_v**2))*(K0_q/delta_v**2 + 2*
    K1_p/(R*delta_v))/(I0_q/delta_v**2 - 2*I1_p/(R*delta_v)))/(-K0_q*(delta_v**2/2
    + 0.5*delta_v**2/bet**2)/delta_v**4 - K1_p/(R*bet**2*delta_v) - K1_q/(R*bet*
    delta_v) - (K0_q/delta_v**2 + 2*K1_p/(R*delta_v))*(-I0_q*(delta_v**2/2 + 0.5*
    delta_v**2/bet**2)/delta_v**4 + I1_p/(R*bet**2*delta_v) + I1_q/(R*bet*delta_v))
    /(I0_q/delta_v**2 - 2*I1_p/(R*delta_v))) + 1 + (K0_p/(2*delta_v**2)
    - K0_q/(2*delta_v**2) - (I0_p/(2*delta_v**2) - I0_q/(2*delta_v**2))*(K0_q/
    delta_v**2 + 2*K1_p/(R*delta_v))/(I0_q/delta_v**2 - 2*I1_p/(R*delta_v)))*(-I0_q
    *(delta_v**2/2 + 0.5*delta_v**2/bet**2)/delta_v**4 + I1_p/(R*bet**2*delta_v) +
    I1_q/(R*bet*delta_v))/((I0_q/delta_v**2 - 2*I1_p/(R*delta_v))*(-K0_q*(delta_v
    **2/2 + 0.5*delta_v**2/bet**2)/delta_v**4 - K1_p/(R*bet**2*delta_v) - K1_q/(R*
    bet*delta_v) - (K0_q/delta_v**2 + 2*K1_p/(R*delta_v))*(-I0_q*(delta_v**2/2 +
    0.5*delta_v**2/bet**2)/delta_v**4 + I1_p/(R*bet**2*delta_v) + I1_q/(R*bet*
    delta_v))/(I0_q/delta_v**2 - 2*I1_p/(R*delta_v))))
50
51 print(simplify(Pi_p))
52
53 #PRESSURE
54 #####
55
56 print(solve_linear_system_LU(Matrix([ [ -(delta_v**2)/((bet*R)**2), (delta_v**2)/2,
    I1_q/(delta_v*bet*R), -K1_q/(delta_v*bet*R), 0,0], [0, delta_v**2, I0_q/(
    delta_v**2), K0_q/(delta_v**2), 0,0], [(delta_v**2)/(R**2), -(delta_v**2)/2, -
    I1_p/(R*delta_v), K1_p/(R*delta_v), 1,0], [1/(R**2), 1/2, I1_p/(delta_v**3*R),
    -K1_p/(delta_v**3*R), 0,1], [-(2*delta_v**2)/(R**3), 0, I1_p/(delta_v**3) -I2_p
    /(delta_v**2*R), -K1_p/(delta_v**3)-K2_p/(delta_v**2*R), 0 , 0]]),[c_0,c_1,c_2,
    c_3,Pi]))
57
58 Pi_p= (delta_v**2*(-I0_q/(R*delta_v**2) + I1_p/delta_v**3 + 2*I1_p/(R**2*delta_v) -
    I2_p/(R*delta_v**2))/(I0_q/delta_v**2 - 2*I1_p/(R*delta_v)) - (delta_v**2*(-
    I0_q*(delta_v**2/2 + 0.5*delta_v**2/bet**2)/delta_v**4 + I1_p/(R*bet**2*delta_v
    ) + I1_q/(R*bet*delta_v))/(I0_q/delta_v**2 - 2*I1_p/(R*delta_v)) + delta_v**2/
    bet**2)*(-K0_q/(R*delta_v**2) - K1_p/delta_v**3 - 2*K1_p/(R**2*delta_v) - K2_p
    /(R*delta_v**2) - (K0_q/delta_v**2 + 2*K1_p/(R*delta_v))*(-I0_q/(R*delta_v**2)
    + I1_p/delta_v**3 + 2*I1_p/(R**2*delta_v) - I2_p/(R*delta_v**2))/(I0_q/delta_v
    **2 - 2*I1_p/(R*delta_v)))/(-K0_q*(delta_v**2/2 + 0.5*delta_v**2/bet**2)/
    delta_v**4 - K1_p/(R*bet**2*delta_v) - K1_q/(R*bet*delta_v) - (K0_q/delta_v**2
    + 2*K1_p/(R*delta_v))*(-I0_q*(delta_v**2/2 + 0.5*delta_v**2/bet**2)/delta_v**4
    + I1_p/(R*bet**2*delta_v) + I1_q/(R*bet*delta_v))/(I0_q/delta_v**2 - 2*I1_p/(R*
    delta_v))) + 2*delta_v**2/R)/((-I0_q*(delta_v**2/2 + 0.5*delta_v**2/bet**2)/
    delta_v**4 + I1_p/(R*bet**2*delta_v) + I1_q/(R*bet*delta_v))*(-K0_q/(R*delta_v
    **2) - K1_p/delta_v**3 - 2*K1_p/(R**2*delta_v) - K2_p/(R*delta_v**2) - (K0_q/
    delta_v**2 + 2*K1_p/(R*delta_v))*(-I0_q/(R*delta_v**2) + I1_p/delta_v**3 + 2*
    I1_p/(R**2*delta_v) - I2_p/(R*delta_v**2))/(I0_q/delta_v**2 - 2*I1_p/(R*delta_v
    )))/((I0_q/delta_v**2 - 2*I1_p/(R*delta_v))*(-K0_q*(delta_v**2/2 + 0.5*delta_v
    **2/bet**2)/delta_v**4 - K1_p/(R*bet**2*delta_v) - K1_q/(R*bet*delta_v) - (K0_q
    /delta_v**2 + 2*K1_p/(R*delta_v))*(-I0_q*(delta_v**2/2 + 0.5*delta_v**2/bet**2)
    /delta_v**4 + I1_p/(R*bet**2*delta_v) + I1_q/(R*bet*delta_v))/(I0_q/delta_v**2
    - 2*I1_p/(R*delta_v))) - (-I0_q/(R*delta_v**2) + I1_p/delta_v**3 + 2*I1_p/(R
    **2*delta_v) - I2_p/(R*delta_v**2))/(I0_q/delta_v**2 - 2*I1_p/(R*delta_v)))

```

```

59
60 print(simplify(Pi_p))
61
62 #Zero vorticity hypothesis
63 #####
64
65 print(solve_linear_system_LU(Matrix([ [ -delta_v**2/(bet*R)**2, delta_v**2/2, I1_q
    /(delta_v*bet*R), -K1_q/(delta_v*bet*R), 0,0], [0, delta_v**2, I0_q/delta_v**2,
    K0_q/delta_v**2, 0,0], [delta_v**2/R**2, -delta_v**2/2, -I1_p/(R*delta_v),
    K1_p/(R*delta_v), 1,0], [1/R**2, 1/2, I1_p/(delta_v**3*R), -K1_p/(delta_v**3*R)
    , 0,1], [0,0, I1_p/delta_v**3, -K1_p/delta_v**3, 0,0]]),[c_0,c_1,c_2,c_3,Pi]))
66
67 Pi_z = (delta_v**2*(-I0_q/(R*delta_v**2) + I1_p/delta_v**3 + 2*I1_p/(R**2*delta_v)
    - I2_p/(R*delta_v**2))/(I0_q/delta_v**2 - 2*I1_p/(R*delta_v)) - (delta_v**2*(-
    I0_q*(delta_v**2/2 + 0.5*delta_v**2/bet**2)/delta_v**4 + I1_p/(R*bet**2*delta_v
    ) + I1_q/(R*bet*delta_v))/(I0_q/delta_v**2 - 2*I1_p/(R*delta_v)) + delta_v**2/
    bet**2)*(-K0_q/(R*delta_v**2) - K1_p/delta_v**3 - 2*K1_p/(R**2*delta_v) - K2_p
    /(R*delta_v**2) - (K0_q/delta_v**2 + 2*K1_p/(R*delta_v))*(-I0_q/(R*delta_v**2)
    + I1_p/delta_v**3 + 2*I1_p/(R**2*delta_v) - I2_p/(R*delta_v**2))/(I0_q/delta_v
    **2 - 2*I1_p/(R*delta_v)))/(-K0_q*(delta_v**2/2 + 0.5*delta_v**2/bet**2)/
    delta_v**4 - K1_p/(R*bet**2*delta_v) - K1_q/(R*bet*delta_v) - (K0_q/delta_v**2
    + 2*K1_p/(R*delta_v))*(-I0_q*(delta_v**2/2 + 0.5*delta_v**2/bet**2)/delta_v**4
    + I1_p/(R*bet**2*delta_v) + I1_q/(R*bet*delta_v))/(I0_q/delta_v**2 - 2*I1_p/(R*
    delta_v))) + 2*delta_v**2/R)/((-I0_q*(delta_v**2/2 + 0.5*delta_v**2/bet**2)/
    delta_v**4 + I1_p/(R*bet**2*delta_v) + I1_q/(R*bet*delta_v))*(-K0_q/(R*delta_v
    **2) - K1_p/delta_v**3 - 2*K1_p/(R**2*delta_v) - K2_p/(R*delta_v**2) - (K0_q/
    delta_v**2 + 2*K1_p/(R*delta_v))*(-I0_q/(R*delta_v**2) + I1_p/delta_v**3 + 2*
    I1_p/(R**2*delta_v) - I2_p/(R*delta_v**2))/(I0_q/delta_v**2 - 2*I1_p/(R*delta_v
    )))/((I0_q/delta_v**2 - 2*I1_p/(R*delta_v))*(-K0_q*(delta_v**2/2 + 0.5*delta_v
    **2/bet**2)/delta_v**4 - K1_p/(R*bet**2*delta_v) - K1_q/(R*bet*delta_v) - (K0_q
    /delta_v**2 + 2*K1_p/(R*delta_v))*(-I0_q*(delta_v**2/2 + 0.5*delta_v**2/bet**2)
    /delta_v**4 + I1_p/(R*bet**2*delta_v) + I1_q/(R*bet*delta_v))/(I0_q/delta_v**2
    - 2*I1_p/(R*delta_v)))) - (-I0_q/(R*delta_v**2) + I1_p/delta_v**3 + 2*I1_p/(R
    **2*delta_v) - I2_p/(R*delta_v**2))/(I0_q/delta_v**2 - 2*I1_p/(R*delta_v)))
68
69 print(simplify(Pi_z))

```

Listing C.1: Code B

## Appendix D

# Code C - Low Frequency Signal (Visco-inertial effects)

```
1 from sympy import *
2
3 init_session()
4 init_printing()
5
6 from sympy import *
7 import numpy as np
8 import scipy.integrate as integrate
9 import scipy.special as special
10
11 omega = symbols('omega',real=True, positive=True)
12 R_f = symbols('R_f',real=True, positive=True)
13 phi = symbols('phi',real=True, positive=True)
14 rho_0 = symbols('rho_0',real=True, positive=True)
15 mu = symbols('mu',real=True, positive=True)
16 lambda_0 = symbols('lambda_0',real=True, positive=True)
17 C_p = symbols('C_p',real=True, positive=True)
18 delta_v = sqrt(mu/(I*rho_0*omega))
19 theta = symbols('theta')
20 iota = symbols('iota')
21 sigma = symbols('sigma')
22
23 bet = sqrt(1-phi)
24 R = R_f/bet
25 p = R/delta_v
26 q = p*bet
27
28 A = -log(bet) -p**2*(phi/4+(2-phi)*log(bet)/4)
29 B=bet*p*log(bet)/2
30 C=p*log(bet)/2
31 E=1/p
32 F=2/(bet*p)
33 G=-phi/(2*bet)
34
35 Pi_v=delta_v**2*(R**2*phi*A+2*R*delta_v*(C-bet*B))/(R**2*(2-phi)*A+2*R*delta_v*(C+
    bet*(2*B-F))+4*R*bet**2*delta_v*E-8*bet*delta_v**2*G)
36 simplify(Pi_v)
37
38 Pi_z=delta_v**2*(R*phi*E+2*bet*delta_v*G)/(R*(2-phi)*E-2*B*delta_v*G)
39 simplify(Pi_z)
```

Listing D.1: Code C

## Appendix E

# Code D - Low Frequency Signal (Thermal effects)

```
1 from sympy import *
2
3 init_session()
4 init_printing()
5
6 from sympy import *
7 import numpy as np
8 import scipy.integrate as integrate
9 import scipy.special as special
10
11 omega = symbols('omega',real=True, positive=True)
12 R_f = symbols('R_f',real=True, positive=True)
13 phi = symbols('phi',real=True, positive=True)
14 rho_0 = symbols('rho_0',real=True, positive=True)
15 mu = symbols('mu',real=True, positive=True)
16 lambda_0 = symbols('lambda_0',real=True, positive=True)
17 C_p = symbols('C_p',real=True, positive=True)
18
19 delta_t = sqrt(lambda_0/(I*C_p*rho_0*omega))
20 bet = sqrt(1-phi)
21 R = R_f/bet
22 p2 = R/delta_t
23
24 Xi=delta_t**2*(1+delta_t**2/(1-p2**2*log(bet*p2)/2))
25
26 Xi_0=re(Xi)
27
28 simplify(Xi_0)
```

Listing E.1: Code D